RIVM report 711401010

**Nitrate Transport Modeling in Deep Aquifers.
Comparison between Model Results and Data
from the Groundwater Monitoring Network**

G.J.M. Uffink and P.F.A.M. Römkens*

February 2001

*) Present address:
 Alterra, Wageningen

RIVM, P.O. Box 1, 3720 BA Bilthoven, telephone: 31 - 30 - 274 91 11; telefax: 31 - 30 - 274 29 71,
 e-mail Gerard.Uffink@rivm.nl

Mailing list

1   drs. J.A. Suurland

2   H.A.P.M. Pont

3   prof. ir. N.D. Van Egmond

4   ir. F. Langeweg

5   ir. R. van den Berg

6   ing. G.P. Beugelink

7   ir. L.J.M. Boumans

8   ir. A.H.M. Bresser

9   dr. ir. J.J.B. Bronswijk

10   ir. G. van Drecht

11   dr. ir. J.J.M. van Grinsven

12   ir. B.J. de Haan

13   drs. H. van den Heiligenberg

14   ir. K. Kovar

15   drs. F.J. Kragt

16   ir. A.M.A. van der Linden

17   W. Ligtvoet

18   dr. ir. C.R. Meinardi

19   ir. J.H.C. Mülschlegel

20   drs. G.B.J. Overbeek

21   ir. M.J.H. Pastoors

22   dr. H.F.R. Reijnders

23   ir. F.J. Sauter

24   dr. ir. A. Tiktak

25   drs. F.G. Wortelboer

26   prof. dr. ir. C. van den Akker, Technische Universiteit, Delft

27   dr. P.J.T. van Bakel, SC-DLO, Wageningen

28   dr. O. Batelaan, Vrije Universiteit Brussel, Belgie

29   ir. C.G.E.M. van Beek, Kiwa, Nieuwegein

30   ir. H. Boukes, Adviesburo Harry Boukes, De Meern

31   ir. J. Griffioen, NITG-TNO, Utrecht

32   prof. dr. W. Kinzelbach, ETH, Zurich

33   drs. G.J.W. Krajenbrink, Waterleiding Laboratorium Oost, Doetinchem

34   dr. ir. W. de Lange, RIZA, Lelystad

Abstract

Nitrate measurements from the Netherlands Groundwater Monitoring Network and model simulations were compared for deep aquifers in the eastern part of the Netherlands. The area studied measured 40 x 30 km^2. The model describes advective-dispersive solute transport in groundwater and utilizes a first-order decay process in a simplified approach to denitrification. On the basis of preliminary model runs several modifications of the solute transport model were proposed; the model was evaluated and discussed after a second series of runs. A major factor in the results appears to be the vertical distribution of the nitrate content and the processes that affect it, such as the vertical mixing by dispersion and the distribution of the downward groundwater velocity. With respect to the denitrification parameter, the best results were obtained with a half-lifetime (T_{50}) between 3 - 5 years and a local refinement underneath the river valleys and brooks, and in a zone above and below the clay layers. The refinement consisted of a further reduction of the half-lifetime based on the presence of organic matter increasing the denitrification capacity. The report further discusses the representativeness in space of the monitoring data and the simulation results.

Contents

Appendices

Samenvatting

Gedurende de laatste decennia heeft intensivering van de veehouderij in Nederland een aanmerkelijke belasting van bodem en water met nutriënten tot gevolg gehad. Dit heeft onder meer geleid tot een verhoging van het nitraatgehalte in het grondwater. In enkele gevallen wordt de EU drinkwaternorm (50 mg L^{-1} NO_3) overschreden, ook in het diepe grondwater (circa 10 meter). Om de grondwaterkwaliteit te bewaken werd gedurende de periode 1979-1984 een Landelijk Meetnet Grondwaterkwaliteit (LMG) ingericht. De meetnetputten worden jaarlijks bemonsterd op verschillende filterdiepten. Het landelijk meetnet heeft onze kennis over de variatie van het nitraatgehalte in ruimte en tijd weliswaar vergroot, maar de dichtheid van de meetpunten is in een aantal gebieden niet altijd voldoende voor uitspraken op lokale schaal. Een simulatiemodel kan hier belangrijke additionele informatie leveren. Simulatiemodellen zijn echter onmisbaar bij de evaluatie van nieuwe beleidsbeslissingen. Hierbij is men immers geïnteresseerd in *toekomstige* veranderingen in de grondwaterkwaliteit. De gegevens van het meetnet verschaffen slechts informatie over de *huidige* toestand van de grondwaterkwaliteit.

In principe kunnen simulatiemodellen een toekomstverwachting geven voor de veranderingen in het nitraatgehalte. Deze modellen dienen rekening te houden met de fysische (transport) eigenschappen van het modelgebied in verband met de verspreiding van nitraat, maar ook met bodemchemische eigenschappen in verband met het afbraakproces (denitrificatie). Onlangs is bij het RIVM een grondwater model (LGMCAD) gereed gekomen dat advectief en dispersief transport van opgeloste stoffen beschrijft en een eerste-orde afbraak (Uffink, 1996, 1999). Een eerste-orde afbraakproces kan, als een eenvoudige benadering, worden gebruikt voor het modelleren van denitrificatie (Wendland, 1992; Van Beek et al., 1994). Het doel van de huidige studie is om de functionaliteit van dit model te onderzoeken en het model daar waar nodig aan te passen. Daartoe is het model toegepast op een studiegebied in oost Nederland (40×30 km^2). Dit gebied is representatief voor de droge zandgebieden waar de nitraatgehaltes de afgelopen decennia sterk zijn gestegen. Ter verificatie van de rekenresultaten zijn deze voor het jaar 1995 vergeleken met gegevens van het Landelijk Meetnet Grondwaterkwaliteit.

Als invoer voor het transport model zijn nodig de hoeveelheden nitraat die infiltreren aan maaiveld. Hiervan bestaan geen meetgegevens. Voor deze studie is gebruik gemaakt van berekende gegevens die werden verkregen door Van Drecht en Scheper (1998) met het model NLOAD. Voor bos en stedelijk gebied zijn deze gegevens aangevuld door Boumans en Van Drecht (1998) aan de hand van een statistische analyse.

Op grond van de resultaten van een reeks voorbereidende berekeningen is een aantal aanpassingen aan het transportmodel voorgesteld. Bij een tweede serie berekeningen zijn de aanpassingen nader onderzocht en besproken. Een belangrijk punt is de verticale verdeling van het nitraatgehalte en de processen die daarop van invloed zijn. De steile verticale concentratiegradiënt kan slechts met het rekenmodel worden gereproduceerd wanneer de verticale dispersie wordt gereduceerd tot het niveau van moleculaire diffusie. Dikwijls laten

grondwatertransportmodellen het gebruik van een dergelijke lage waarde voor de dispersiviteit niet toe zonder dat er complicaties optreden (numerieke dispersie). In het hier toegepaste model (LGMCAD) blijft numerieke dispersie achterwege, aangezien LGMCAD is gebaseerd op een zgn. Lagrange-benadering (particle-tracking). Er wordt verder aandacht besteed aan de verticale advectieve stromingscomponent. De lineaire verdeling die volgt uit de benadering van Dupuit-Forchheimer is vervangen door een parabolische verdeling, omdat deze meer recht doet aan het feit dat bij verticale stroming enige weerstand moet worden overwonnen.

Wat betreft de denitrificatieparameter werd de beste overeenkomst tussen metingen en modeluitkomsten verkregen bij een halfwaardetijd (T_{50}) van 3 tot 5 jaar. Plaatselijk, dwz in de buurt van de beekdalen en andere waterlopen en in een zone boven en onder de kleilagen, is gekozen voor een kleinere halfwaardetijd. Dit is gebaseerd op de aanwezigheid van organische stof, hetgeen de denitrificatie bevordert.

Tenslotte wordt in het rapport kort ingegaan op de ruimtelijk representativiteit van de berekeningen en hoe deze kan worden beïnvloed door de modelgebruiker. Veelal bestaat er een aanzienlijke discrepantie tussen de ruimtelijke representativiteit van berekeningen enerzijds en die van meetgegevens anderzijds. In de huidige studie hebben de modelresultaten betrekking op een blok van circa honderd meter horizontale richting en enkele meters in verticale zin. Het representatieve volume van de metingen is echter zeer beperkt en ligt in de orde van grootte van 10 - 15 liter. In hoeverre de genoemde discrepantie van invloed is geweest op de gevonden parameterwaarden is in dit rapport niet nader onderzocht. Dit onderwerp verdient wellicht nadere aandacht.

Het huidige rekenmodel is een geschikt gereedschap voor het maken van landsdekkende beelden van de nitraatconcentratie in het grondwater. Voorwaarde daarbij is dat ook voor de overige deelgebieden van Nederland vergelijkende studies tussen modeluitkomsten en waargenomen nitraatgehaltes worden uitgevoerd volgens de in dit rapport beschreven procedure. Op deze wijze dient te worden na te gaan in hoeverre de in dit rapport gevonden afbraakparameters elders toepasbaar zijn.

Summary

During the last few decades intensification of animal husbandry in the Netherlands has led to a significant burdening of soil and water with nutrients. This has led to the rise of groundwater nitrate levels. In some cases the EU drinking water standard (50 mg L^{-1} NO$_3$) is exceeded, also in the deeper groundwater at depths of circa 10 meters. A National Groundwater Monitoring Network was installed during 1979-1984 to monitor the groundwater quality. At present samples are collected annually in the monitoring wells at various filter depths. The monitoring network has improved our understanding of the spatial and temporal variation of nitrate, but in a number of cases the density of the sample points is still insufficient for answers to local scale problems. Here, a simulation model may provide important additional information. However, simulation models are essential to evaluate policy decisions made today. In this case one is interested in *future* changes in the groundwater quality, while the monitoring network provides information only on the *present* state of the groundwater quality.

In principle simulation models may predict changes of nitrate content. These models must take into account the physical (transport) properties of the area in connection with the spread of the nitrates through the ground, but also with soil chemical properties in connection with the decay process (denitrification). Recently, at RIVM a groundwater model (LGMCAD) has been completed that describes advective-dispersive transport and includes a first order decay process. First order decay can be used as a simplified approach for denitrification (Wendland, 1992; Van Beek et al., 1994). The aim of the present study is to test the functioning of this transport model and to modify the model if necessary. For this purpose the model has been applied in a study area in the eastern part of the Netherlands (40×30 km^2). This area is representative for the sandy areas where groundwater nitrate contents have increased considerably during the past decades. The model results have been compared with data from the Groundwater Monitoring Network for the year 1995.

Among the input data the model needs are the amounts of nitrate that infiltrate from the ground surface over the period 1950 - 1995. These data were not available from measurements. In this study data have been used that were generated by Van Drecht and Scheper (1998) using the model NLOAD. Boumans and Van Drecht (1998) completed these with data from a statistical analysis for forested and urban regions.

Several modifications to the solute transport model are proposed based on preliminary model runs. In a second series of runs the modifications are evaluated and discussed. A major factor appears to be the vertical distribution of the nitrate content and the processes that affect it. The steep vertical concentration gradients of the field data can only be reproduced when in the model vertical mixing by dispersion is reduced to the level of molecular diffusion. Most groundwater transport models do not allow such low dispersivity values without introducing numerical dispersion or other complications. These complications do not occur in LGMCAD since it is based on a Lagrangian approach (particle tracking). The vertical variation of the

advective flow component is also investigated. The linear distribution, as follows from the Dupuit-Forchheimer approach, has been replaced by a parabolic distribution, since it does more justice to the fact that for vertical flow some resistance has to be overcome. In the Dupuit-Forchheimer approach it is assumed that no resistance exists to vertical flow.

With respect to the denitrification parameter, different values and configurations have been applied, constant over the area and varying in space horizontally and vertically. The spatial pattern for the denitrification parameter is based on the presence of organic matter, which is more likely to occur near clay layers and underneath riverbeds or the beds of secondary streams. The best fit of model results and network data is obtained using a half-life time (T_{50}) between 3 - 5 years while near rivers and brooks and in a zone around the clay layers the half-life time has been reduced to 1 - 2 years.

Finally the report discusses the representativeness of the simulation results and how it may be influenced by the decision of the model user. Generally a considerable discrepancy exists in the representativeness of model results and measurements. In this study the model results refer to blocks of some hundred meters horizontally a few meters vertically, while for the measurements the representative volume is very limited and has an order of magnitude of 10 -15 liters. In this report it has not been examined to what extent the discrepancy mentioned above affects the parameter values found in our study. This subject may need further attention.

The present simulation model is a suitable tool to describe nitrate contents in groundwater on a national scale, provided that for the remaining areas of the Netherlands similar comparative studies are carried out between calculated and observed nitrate contents. The purpose of such studies must be examination whether parameter values found in this report may also be applied to other areas in the country.

1   INTRODUCTION

Groundwater is of interest not only as a source for the production of drinking water. It interacts with larger and smaller surface-waters and, directly or indirectly, affects most aquatic ecosystems. Therefore, groundwater needs to be protected quantitatively as well as qualitatively. During the last few decades, however, an increased surface load of nitrate, mainly due to intensive animal husbandry associated with manure application, led to a significant rise of groundwater nitrate levels in the southeastern part of the Netherlands. In some cases the EC drinking water standard (50 mg L^{-1} NO_3, or 11 mg L^{-1} NO_3-N) is exceeded.

   During 1979-1984 the National Groundwater Monitoring Network (NGM) was installed in the Netherlands to monitor the groundwater quality (Van Duijvenbooden et al., 1985). At more than 300 sites the groundwater is sampled annually at various depths. It has resulted in groundwater quality maps of the Netherlands for various components including nitrate (Van Drecht et al., 1996). The monitoring network reveals a significant relationship between nitrate concentrations in the groundwater on the one hand and the *N*-load at the earth's surface, the land use and the soil type on the other hand. For instance, little nitrate is found under forest and heath areas, while plumes of nitrate occur under arable areas. The monitoring network has improved our understanding of the spatial distribution and temporal variation of nitrate, but in certain regions the density of the sample points is still low. To some degree, scarcity of data in restricted areas can be overcome by geostatistical methods. Pebesma and De Kwaadsteniet (1994, 1995) and Pebesma (1996) utilize an interpolation technique (block-kriging) to obtain maps for the network data (including nitrate). However, these maps have a rather low horizontal resolution (one data point represents a 4×4 km^2 block), while in the vertical direction only two elevations are distinguished. In Pebesma's method also confidence intervals can be mapped. Areas with a low density of measuring points are characterized by a low degree of confidence (large confidence intervals).

   Simulation models are useful and sometimes essential tools in groundwater quality management problems. In the first place, simulation models may offer additional information where network data maps do not show enough detail. Secondly, models may be helpful in designing or redesigning a monitoring network. However, network data refer only to the present state the groundwater quality as a result of the policy pursued in the past few decades. For the evaluation of newly taken policy measures *future changes* in the nitrate concentration must be known. In order to *predict* spatial and temporal changes in the nitrate concentration, models are needed. Predictive models can be used to evaluate current and future legislative measures for control of nitrate emission. The models must take into account both the physical (transport) and the chemical (denitrification) properties of the region. Reduction of nitrate in *unsaturated soils* is well known and well documented, but less information is available on nitrate reduction in *deep aquifers*. According to Appelo and Postma (1993) denitrification in *deep aquifers* can lead to a significant nitrate reduction. Previous modeling efforts that did not consider denitrification

(Kovar et al., 1996; 1998) have overestimated nitrate concentrations for various drinking water stations.

Recently a groundwater transport model has been completed that describes advective-dispersive solute transport and includes a first order decay process (Uffink, 1996, 1999). First order decay can be utilized as a simplified approach for denitrification (Wendland, 1992; Van Beek et al., 1994). The aim of the present study is to test the functioning of this solute transport model. For this purpose the model is applied in an area in the eastern part of the Netherlands and model results are compared with nitrate measurements from the monitoring network. The comparison is by no means expected to produce a good fit, since the calculation is based on too many, quite rigorous assumptions, simplifications and even pure guesses. In the first place, the hydrological system is treated as a stationary system over the total simulation period (1950 - 1995), while for certain typical dry and wet years have occurred during that period. Furthermore, seasonal fluctuations, which are still felt in the upper zones of the aquifers, are not taken into account by the model. Secondly, for a realistic simulation of the nitrate transport during a certain period it is essential to have data on the amounts of nitrate entering the groundwater system, both spatially distributed as its distribution in time. Such data are rarely, if ever, available from measurements. The best alternative is to use synthetic data, i.e. data generated by other simulation models. Clearly, these synthetic data are subject to additional inaccuracies, simplifications and model 'errors', which all will be inherited by the groundwater transport model. Comparison of model results and data from the monitoring network has been applied only to indicate the model performance. Based on the results of the first series of model runs several modifications have been applied and tested. In a second series of runs these modifications are further evaluated and discussed.

The organization of the report is as follows. Chapter 2 starts with a description of the study area. The geohydrological structure of the area is discussed and the hydrological variables as obtained by the hydrological model are given in a number of contour plots. Special attention is paid to the so-called *Top System* , because of its relevance with respect to the nitrate input at the ground surface. Accordingly the observations from the Groundwater Network are briefly discussed. In Chapter 3 a short introduction on the transport model is given, followed a presentation of the simulation results. First, preliminary results are presented obtained by the model without denitrification. Accordingly, results are presented for a denitrification parameter that is constant over the entire model. In the last section of this Chapter 3 several model refinements are proposed and evaluated. Chapter 4 deals with a discussion of the simulation results obtained with the model refinements. Various aspects such as representativeness and variability of the data are discussed here as well. In Chapter 4 several concluding remarks are made.

2   MATERIAL AND METHODS

2.1   Study Area

The study area, known as 'The Achterhoek', is located in the eastern part of the Netherlands
(Figure 1) and covers an area of 40×30 km^2 (x-coordinates: 200 - 240 km; y-coordinates 435 -
465 km). The area is dominated by a flat or slightly undulating, rolling landscape with a general
elevation between 20 and 25 m in the east and between 10 and 15 m in the west. Figure 2 gives a
topographic map of the area, while Figure 3 gives contours of the surface elevation.
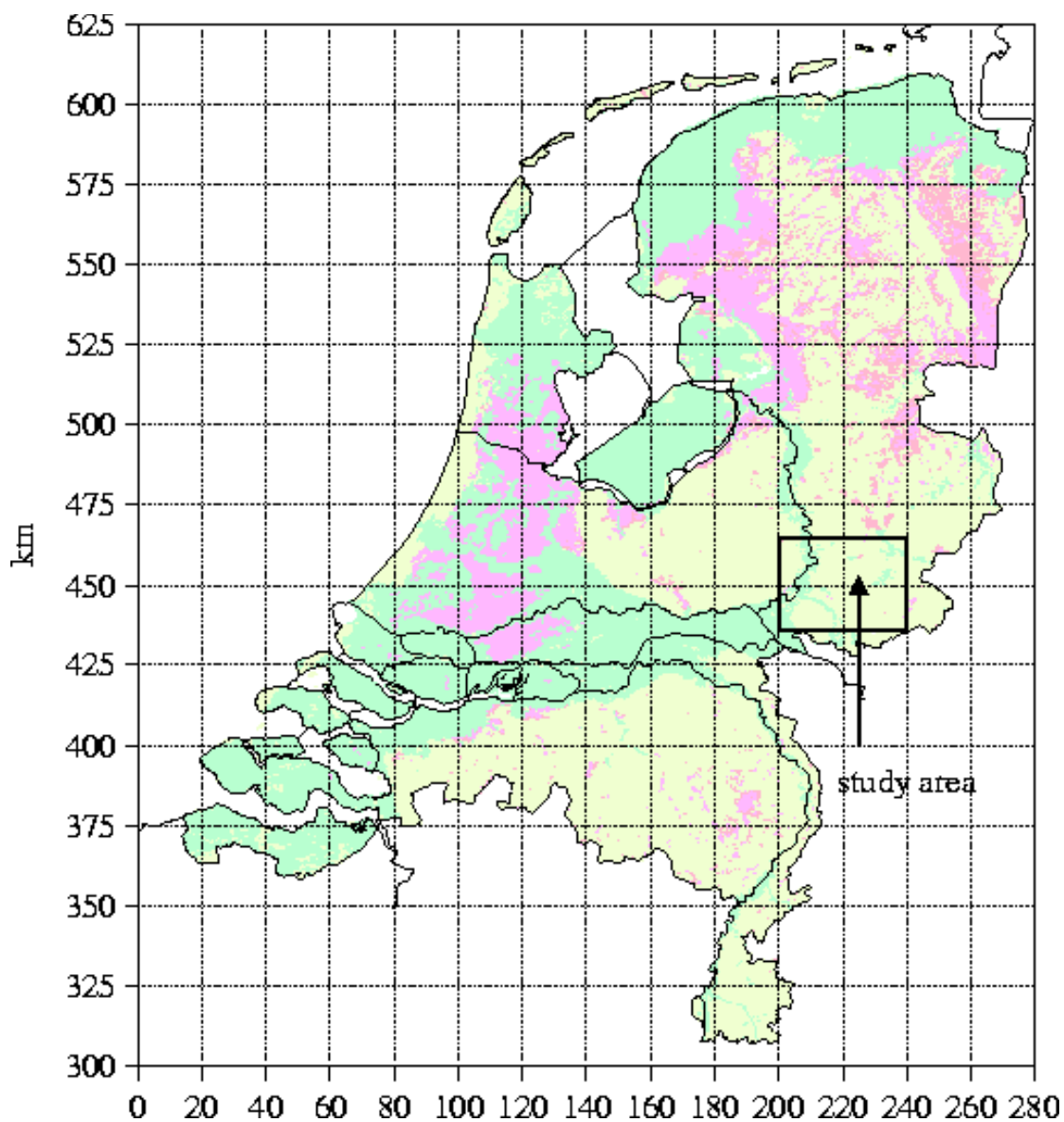
Figure 1. Location of study area 'Achterhoek'. Coordinates in km.

The area is crossed by a number of brooks running from east to west and discharging into the river IJssel (see also Figure 11, section 2.3). Striking elements in the landscape are the 'Lochemerberg' *(a)* in the north and a hilly area known as 'Montferland' *(b)* in the south (Figure 3). Along the western boundary the foothills of the 'Veluwe' *(c)* can be noticed.
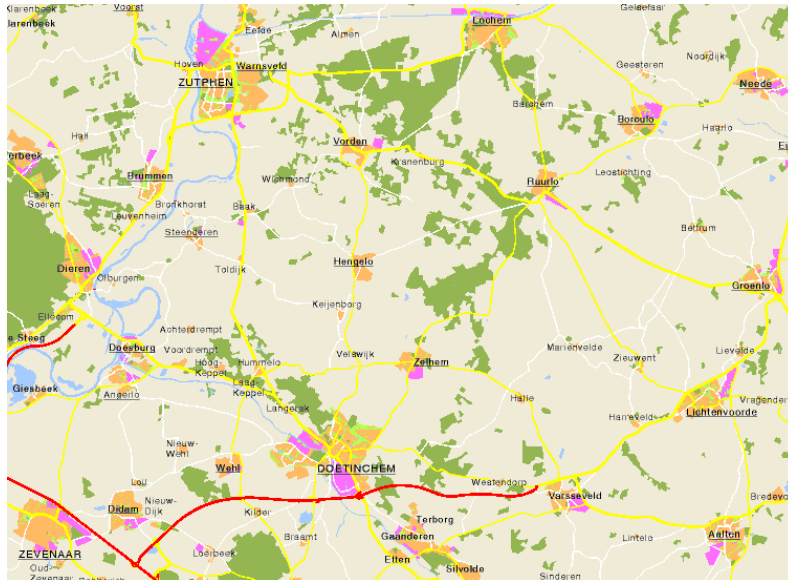
Figure 2. Topography of study area.
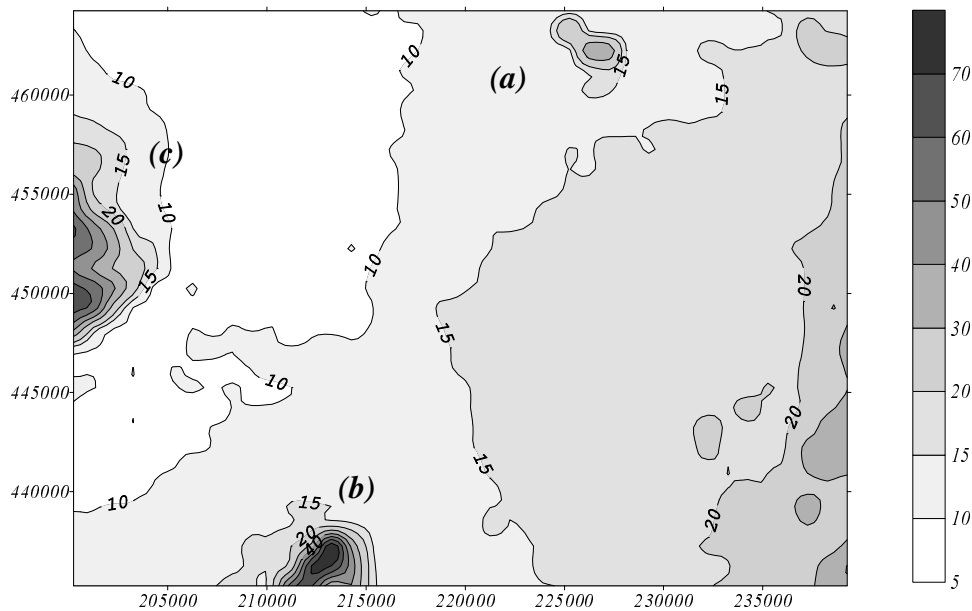
Figure 3. Surface elevation of the study area (in m above NAP). Coordinates in m.

2.2   Aquifer System

The aquifer system consists of a complex of sandy layers from pleistocene origin with a thickness that varies considerably. Along the eastern boundary it varies from 10 to 30 meters, while in the northwest the thickness reaches 220 meters and more. The system is bounded vertically by poorly conductive tertiary sediments of heavy marine clays. This formation, which is considered as impervious, is found in the southeast at a depth of 10 meter above NAP (NAP is the standard reference level in the Netherlands), while it drops downward in the northwest direction to depths of 200 m below NAP and more (Figures 4 and 5). In the western part of the area some semi-pervious clay layers separate the aquifers. In the IJssel valley (northwest) a layer of Eemian clay occurs between 5 m -NAP and 10 m -NAP (Figure 6). The maximum thickness is 5 meters and the hydraulic resistance varies from a few days to 2500 days. A second, more important layer of heavy clay (Drenthe-formation/Tegelen-formation) is present in most of the western part of the area (Figure 7). The depth of this layer varies from 20 m -NAP to 80 m below NAP. In the southwest the thickness is 50 meters. The resistance of the layer is several ten thousand days. More details on the geohydrology of the Achterhoek are found in Grootjans, 1984 and Vermeulen et al., 1996.

Where the clay layers are absent the system acts as a single phreatic aquifer. Groundwater levels are found close to the earth's surface except for the hilly areas. Three vertical cross-sections running in x-direction (Figure 8) show the variation in aquifer thickness and the vertical position of the clay layers mentioned above. The cross-sections denoted as *A-A'*, *B-B'* and *C-C'* are located along the horizontal lines $y = 440000$ m, $y = 450000$ m and $y = 460000$ m, respectively (see Figures 6 and 7).
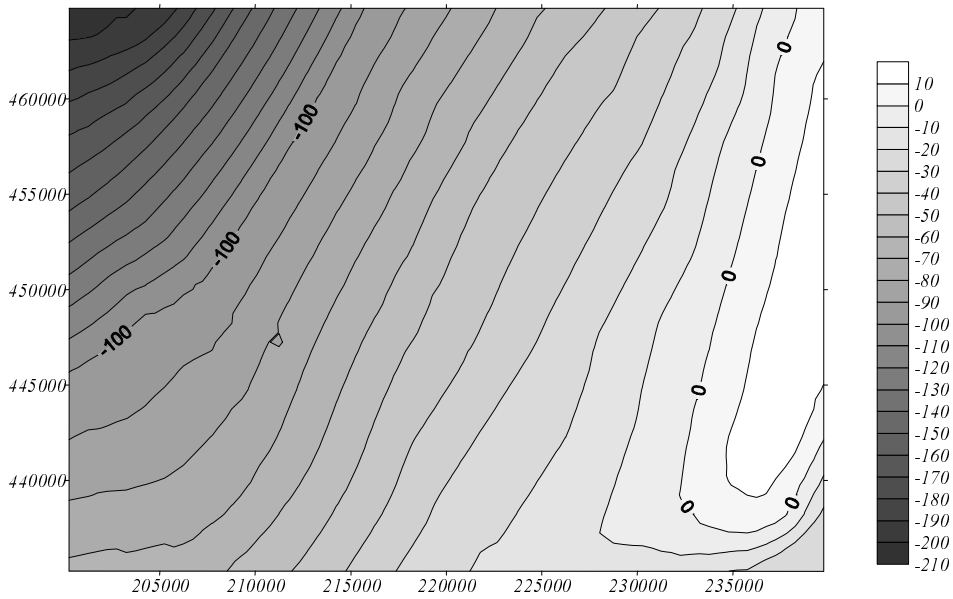
Figure 4. Contours of the base of the aquifer system (in m NAP).
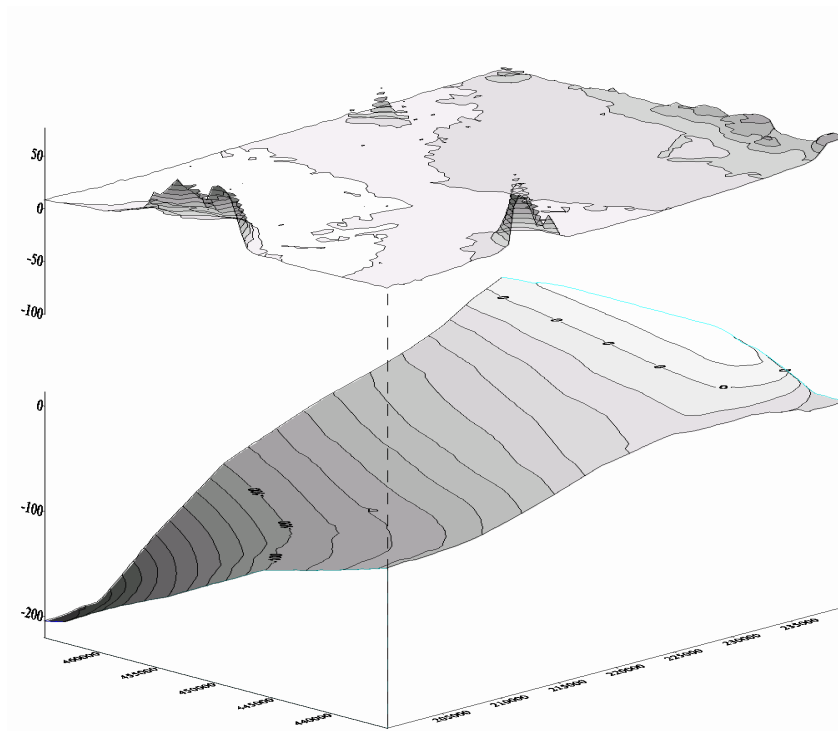
Figure 5. 3D View of top and base of the aquifer system.
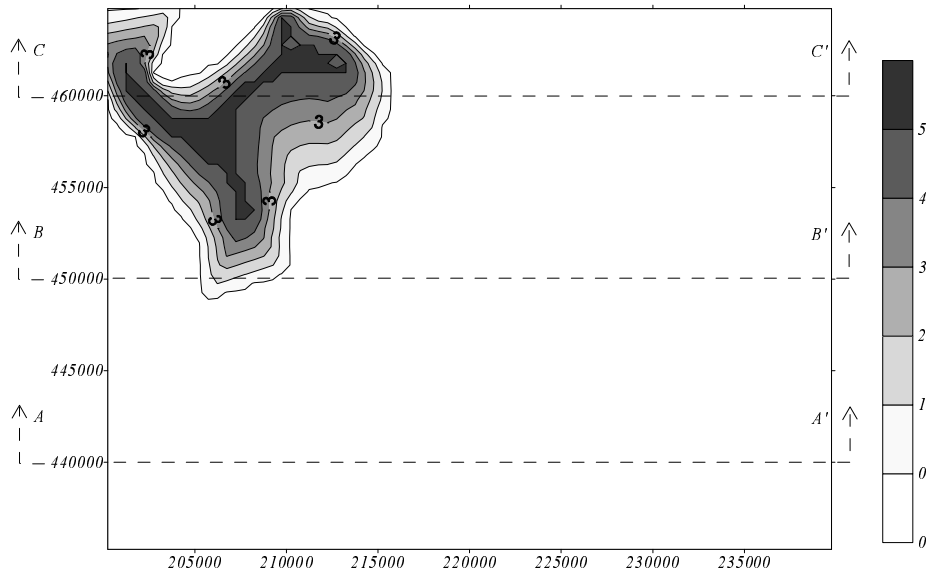
Figure 6. Thickness in meters of upper clay-layer (Eemian clay).
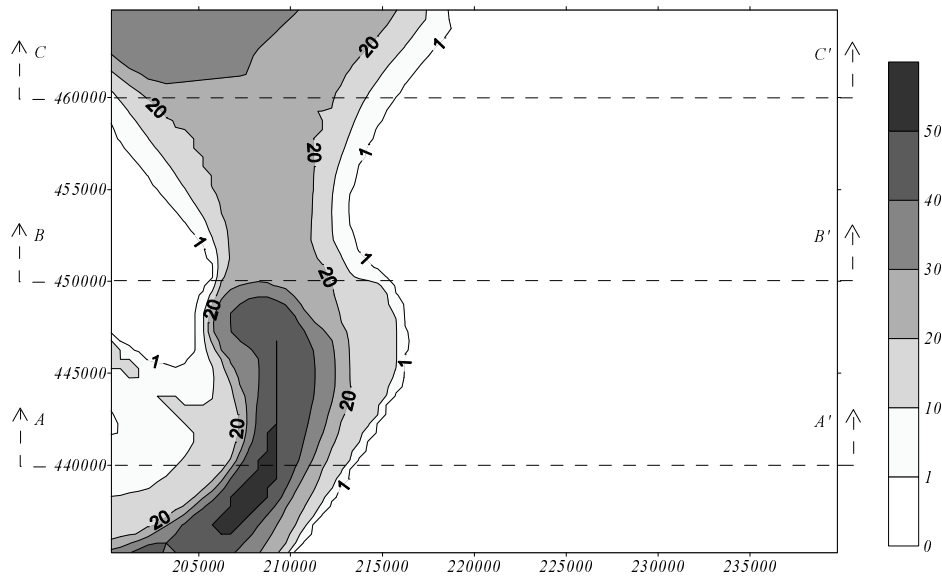
Figure 7. Thickness in meters of second clay-layer (Drenthe-clay).
(Cross-sections A-A', B-B' and C-C' see Fig. 8)
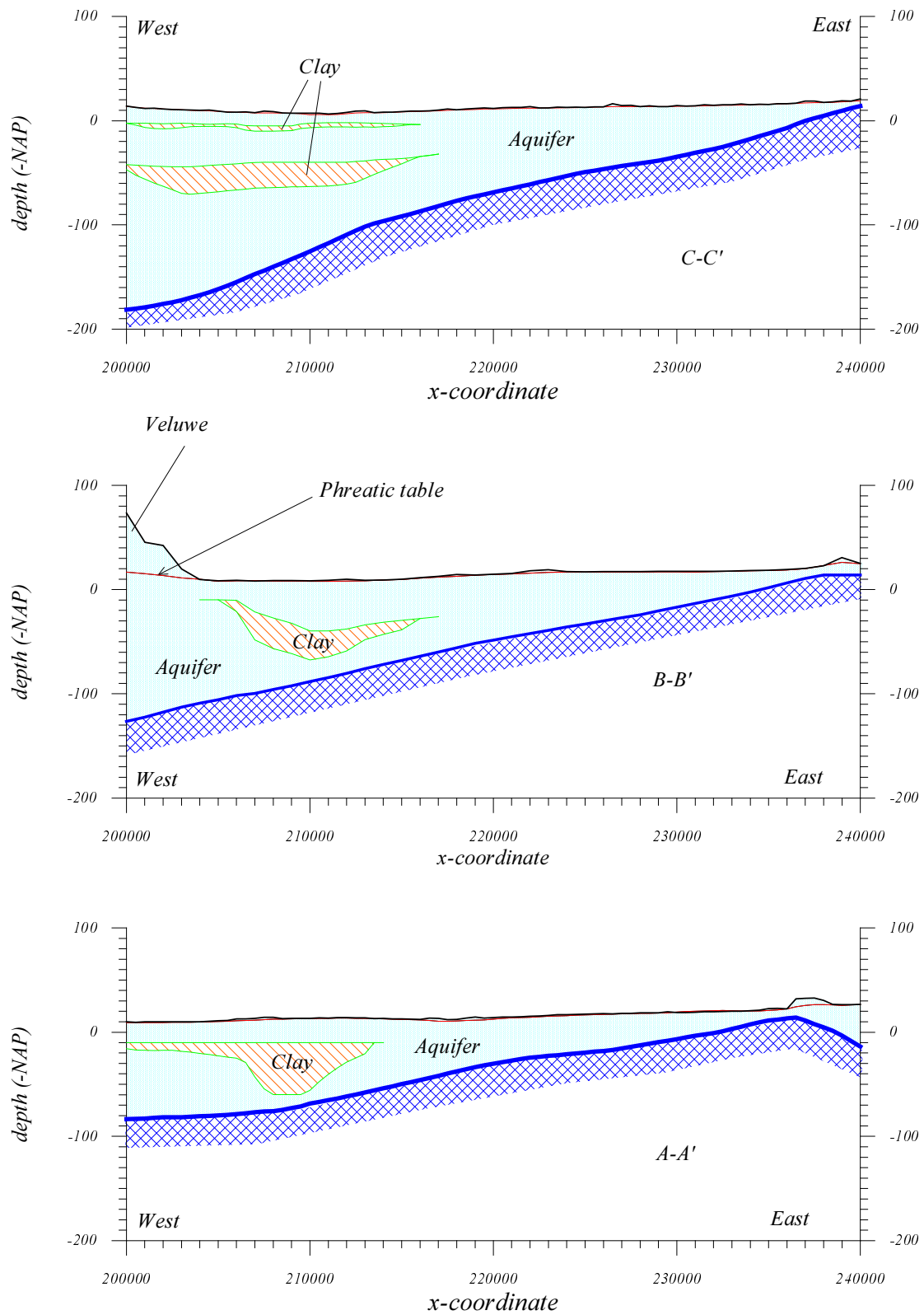
Figure 8. Cross-sections A-A', B-B' and C-C' .

2.3   Groundwater Heads and Velocities

For groundwater heads and velocities, the transport model relies on the hydrological model LGM (National Groundwater Model of the Netherlands). LGM is a finite element model for a multi-aquifer system developed by RIVM (Kovar et al. 1992; Pastoors, 1992). For several parts of the Netherlands, including the 'Achterhoek', hydrological calculations have been carried out with LGM using a 250×250 m^2 element grid (see Kovar et al., 1998). Note that Kovar et al. refer to a model area 'Achterhoek' (model code a2), which is slightly larger than the area in our study.

In principle, the geohydrological system consists of 4 aquifers separated by semi-pervious clay layers. Where the clay layers are absent, the system behaves as a single aquifer. In the present study the groundwater flow is treated as a stationary system under the assumption of constant surface hydraulics and constant groundwater recharge from excess rainfall. In an earlier study the resulting head distribution was calibrated on measured groundwater heads. It has been recognized that for solute transport problems calibration should be on groundwater fluxes, but such a calibration procedure is complicated, if possible at all, and falls beyond the scope of the present study.

Groundwater velocities have been derived from the head distribution by the LGM module LGMFLOW (formerly EFGO). The current section presents some hydrological variables as calculated by LGMFLOW and as applied in the transport module LGMCAD. Figure 9 gives a contour plot of the groundwater surface (phreatic head). This surface mainly follows the relief of the land surface with less pronounced gradients under the hilly sections (compare Figures 2 and 7). Below the clay layers the head differs from the phreatic head, but for the present study the head distribution below the clay layers is not relevant.
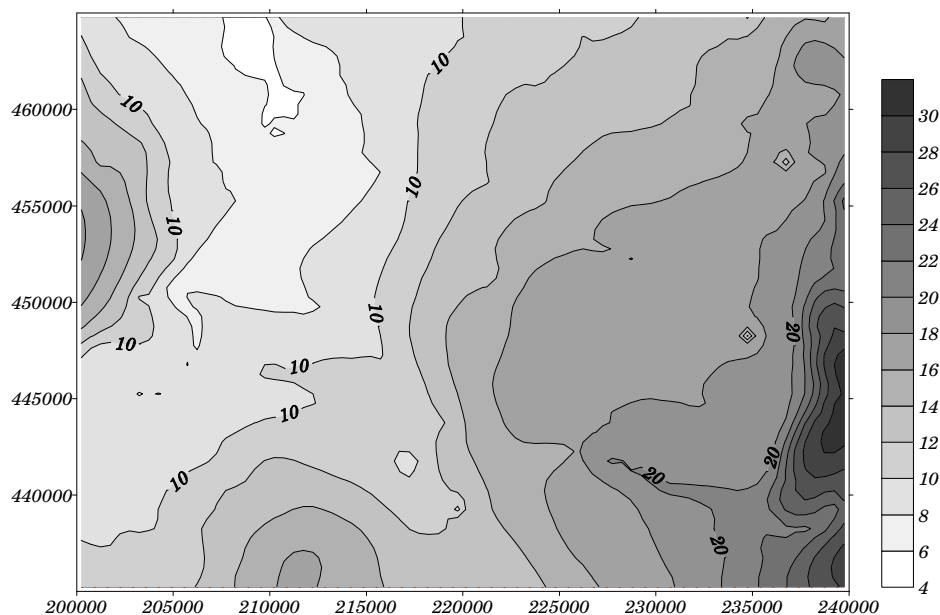
Figure 9. Phreatic surface in meters above NAP.
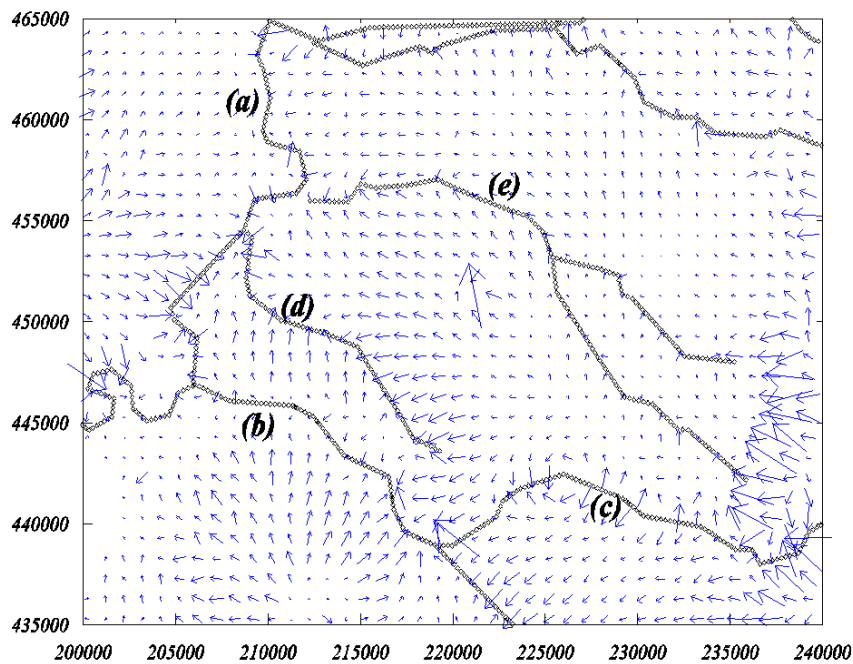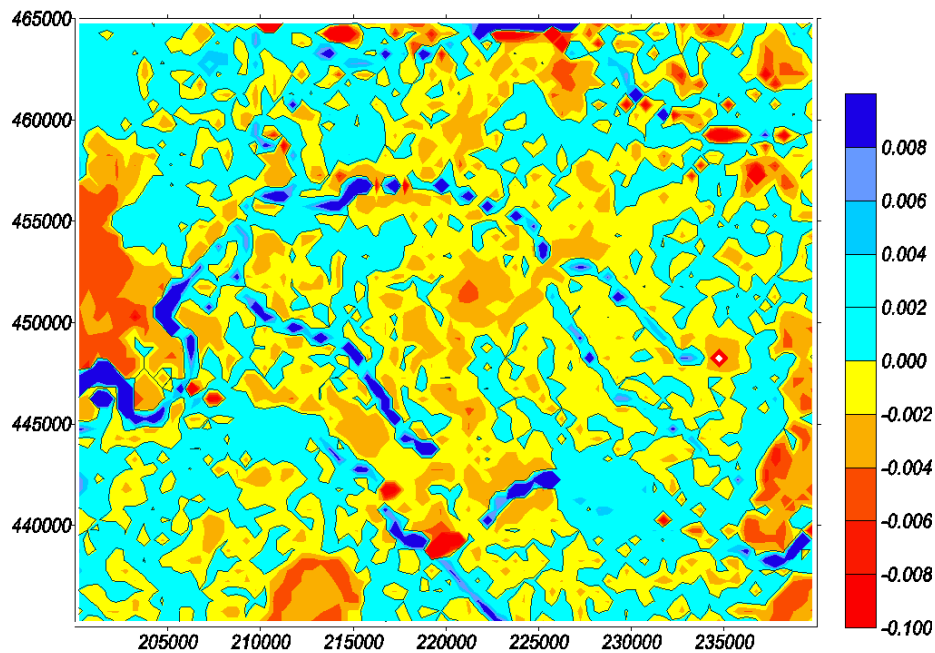
Figure 10 (top).   Vertical velocity. Seepage (cyan to blue) and recharge (yellow to red) Units: meters per day.

Figure 11 (below)   Horizontal velocity. Surface waters: (a) IJssel; (b) Oude IJssel; (c) Slingebeek;(d) Groote Beek; (e) Veengoot.

Figures 10 and 11 show the groundwater velocity distribution at 1 m below the phreatic surface. The **vertical** flow component (in meters per day) is displayed by a color-coded contour map (Figure 10), while the **horizontal** component is presented as a vector plot (Figure 11). The scale of the vector plot is such that the length of the arrows corresponds to an advective displacement of the water during 8000 days (22 years). The vertical flow in the positive z-direction (upward) corresponds to seepage and is indicated by shades of cyan to blue. High seepage rates are found along the rivers (Oude IJssel, Berkel, Slinge, etc). In the hilly areas (Veluwe and Montferland) infiltration occurs (excess rain) resulting in groundwater recharge. Downward flow rates (infiltration) are indicated by shades of yellow to red. As depth increases the vertical flow component gradually decreases until it vanishes at the impervious base. The abnormally high horizontal velocity seen in the center of Figure 11 is due to the presence of the groundwater pumping station *'t Klooster*. The almost radial pattern due to infiltration at the hills of *Montferland* can be clearly observed. Also worth noting is the flow pattern along the draining and infiltrating parts of the brooks. One can see that from the upstream part of the *Slingebeek (c)* water is infiltrating into the aquifer system. This is in line with the remarkable shape of the 20-meter contour in Figure 9. High velocities along the eastern boundary are due to the combined effect of a high infiltration rate and a small aquifer thickness.

2.4   Top System

In the LGM concept the *aquifer system* is completed at the top by a so-called *top-system* (Kovar et al. 1992). This system plays a major role in the distribution of the amount of excess rain into two parts: one part that discharges into the drainage system, and another part that remains underground as groundwater recharge. It also affects the final load of nitrate that reaches the groundwater and, therefore, it needs to be discussed here in a little more detail.

The top system itself represents the zone where interaction takes place between the shallow groundwater and the secondary drainage system of ditches and drains. The water infiltrated at the earth's surface may leave the underground after a very short stay and discharge into the drainage system. In the LGM concept the rate of this discharge depends on the phreatic head. This so-called top system discharge, denoted as q_{ts}, is modeled as a diffusely distributed sink term. Its magnitude follows from a linear relation with the phreatic head φ:

$$q_{ts} = a \, (\varphi\text{-}h_0) \qquad\qquad\qquad (1)$$

Here a is a coefficient of proportionality and h_0 is the so-called zero drainage level. When φ is greater than h_0, the system discharges water, while infiltration occurs when φ is less than h_0. Both h_0 and a may vary in space, so in general q_{ts} is a function of the horizontal coordinates x and y. Thus, the discharge q_{ts} consist of a portion of the recharge that at first enters the aquifer,
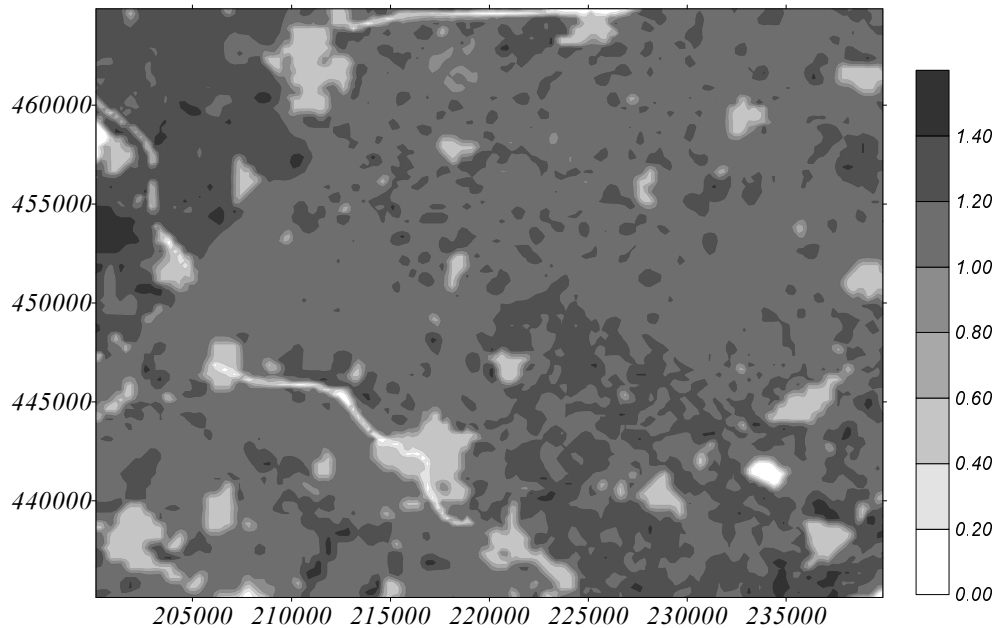
Figure 12. Spatial distribution of annual averaged rain excess (mm/day).

but after a relatively short stay leaves the aquifer again. For the present study the important consideration with respect to the top system is that with the discharge also an amount of nitrates is carried off. The fluxes of nitrate coming in and going out of the top system will be considered later. For the moment we focus on the water fluxes.

As the result of rainfall, surface runoff and evapotranspiration, an amount of water, denoted by q_{re} (*r*ain *e*xcess), enters the aquifer. Figure 12 gives the distribution of q_{re} over the area in mm/day. The distribution reflects the topography of the area (Figure 2 and Figure 3). The light colored areas (little rain excess) coincide with urbanized areas (the cities Zutphen, Doetinchem, Zevenaar, etc). The rain excess enters the groundwater system, but as mentioned earlier, a portion q_{ts} is removed via the top system after a relatively short stay in the aquifer. In the LGM concept this amount is not explicitly modeled, but it is taken into account by the net water flux entering the aquifer system, q_{as}. The flux entering the aquifer becomes the excess rain minus the top-system discharge:

$$q_{as} = q_{re} - q_{ts} \qquad\qquad (2)$$

Note that with respect to the aquifer q_{as} and q_{re} are source terms, while q_{ts} is a sink term. A positive q_{as} leads to a downward (and therefore negative) vertical velocity v_z at the top of the aquifer. The situation as described above becomes slightly different if one of the terms in Eq. (2)

becomes negative. E.g., if q_{ts} is larger than q_{re} it means that the drainage system removes more water than is supplied by rain excess. In that case an additional flux occurs from the aquifer into the drainage system (q_{as} is negative and thus represents a sink term now). The case $q_{ts} < 0$ corresponds with the situation where the drainage system acts as an infiltration system. The final amount of water into the aquifer now consists of the rain excess plus an amount that infiltrates from the drainage system. The flux at the top of the aquifer is always equal to q_{as}, where a positive value means infiltration. Consequently, at the top of the aquifer the following relation holds:

$$q_{as} = -n v_z \qquad (3)$$

where n is the porosity. Note however that Eq. (3) holds only when no additional source or sink terms are present (e.g. from rivers).

Figures 13 and 14 give the distribution of q_{ts} and q_{as}, respectively. Note that sometimes q_{ts} is negative, which means that infiltration into the aquifer occurs instead of discharge. Also note that over a considerable area the drainage term is higher than the actual rain excess. This indicates that, in addition to the rain excess, groundwater from the deeper regions of the aquifer discharges into the drainage system. These areas can be identified in Figure 14 by shades of blue to cyan, corresponding with a negative q_{as}. In those cases the groundwater flux is upward and obviously the nitrate flux **into** the aquifer is zero (more in § 2.6).
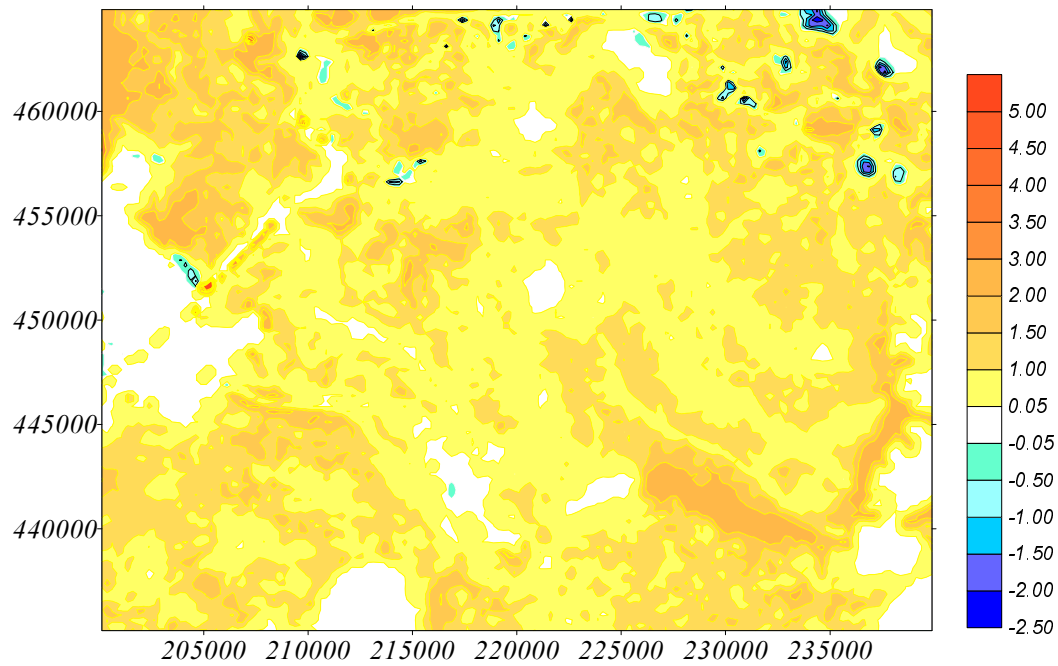
Figure 13. Spatial distribution of discharge into drainage system (q_{ts} in mm/day).
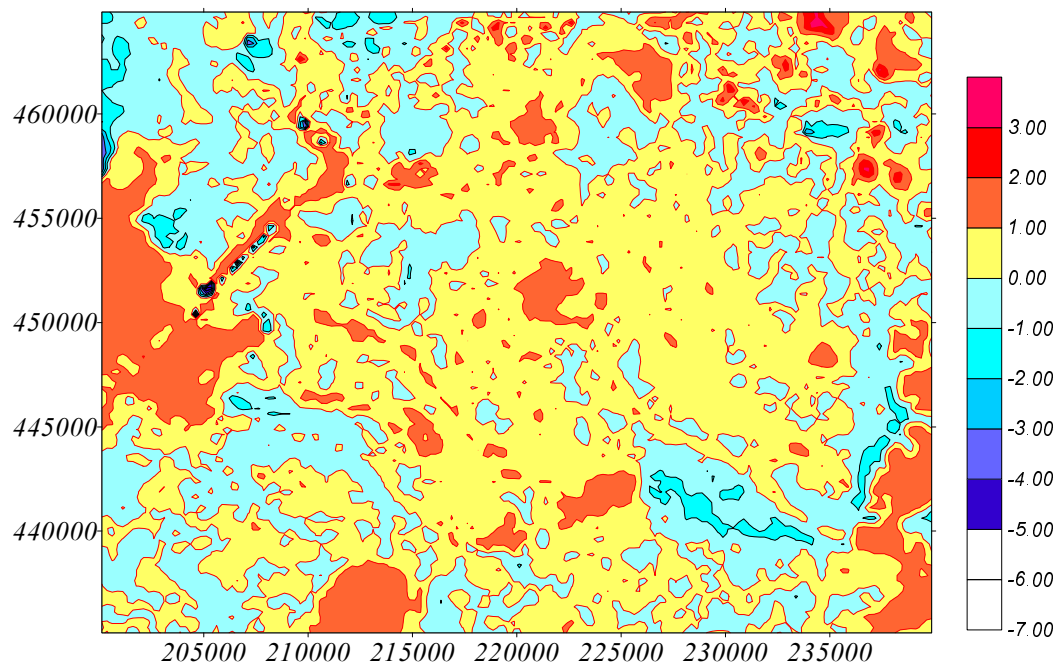
Figure 14. Spatial distribution of groundwater flux into the aquifer system (q_{as} in mm/day).

2.5   Source of Nitrate

The soils in the area are mainly sandy soils except along the river valleys. Especially in the IJssel valley heavy textured soils (silt, clay) as well as peat soils are abundant. The land use is dominated by animal husbandry on grassland, with maize cropping for cattle food. Traditionally, the manure produced by the cattle is applied directly to the maize plots and grassland.

As input the transport model requires data on the amounts of nitrate entering the system. Since measured quantities are not available, generated data have been applied. The leaching rates from agricultural soils have been modeled by Van Drecht et al. (1991) with the model *NLOAD* (also Van Drecht, 1993; Van Drecht and Schepers, 1998). Boumans and Van Drecht (1998) completed these data, that did not cover forested and urban areas, with data from a statistical analysis. A more detailed description of the nitrate leaching data is given by Kovar et al (1998). According to Van Drecht et al. the annual *N*-load has increased from less than 30 kg N ha^{-1} yr^{-1} in the 1950's to more than 1000 kg *N* ha^{-1} yr^{-1} during the 1980's. Figure 15 gives as a function of time the annual amount of nitrate that enters the area. The graph gives the amount integrated over the total study area (total surface is 12 10^8 m^2). Since 1985 restrictions on spreading manure are in effect and at present (1995) the amount of nitrate has decreased compared to the decade '80-'90.

Figure 16 shows the spatial variation of the leaching rate for various moments in time. The spatial variation is due to differences in land use and crop type. The white areas coincide with urbanized areas. The effect of the restrictive measures since the 80's is clearly seen in the plot for 1995.
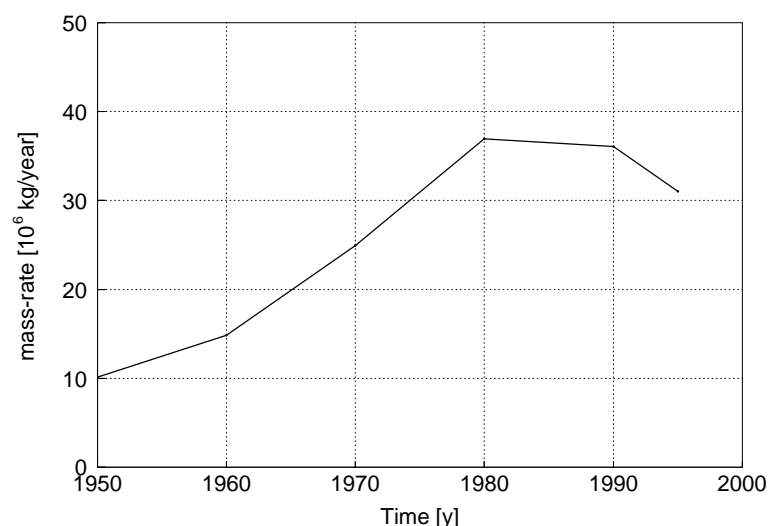
Figure 15. Leached amount of nitrate to groundwater system for the 'Achterhoek'.
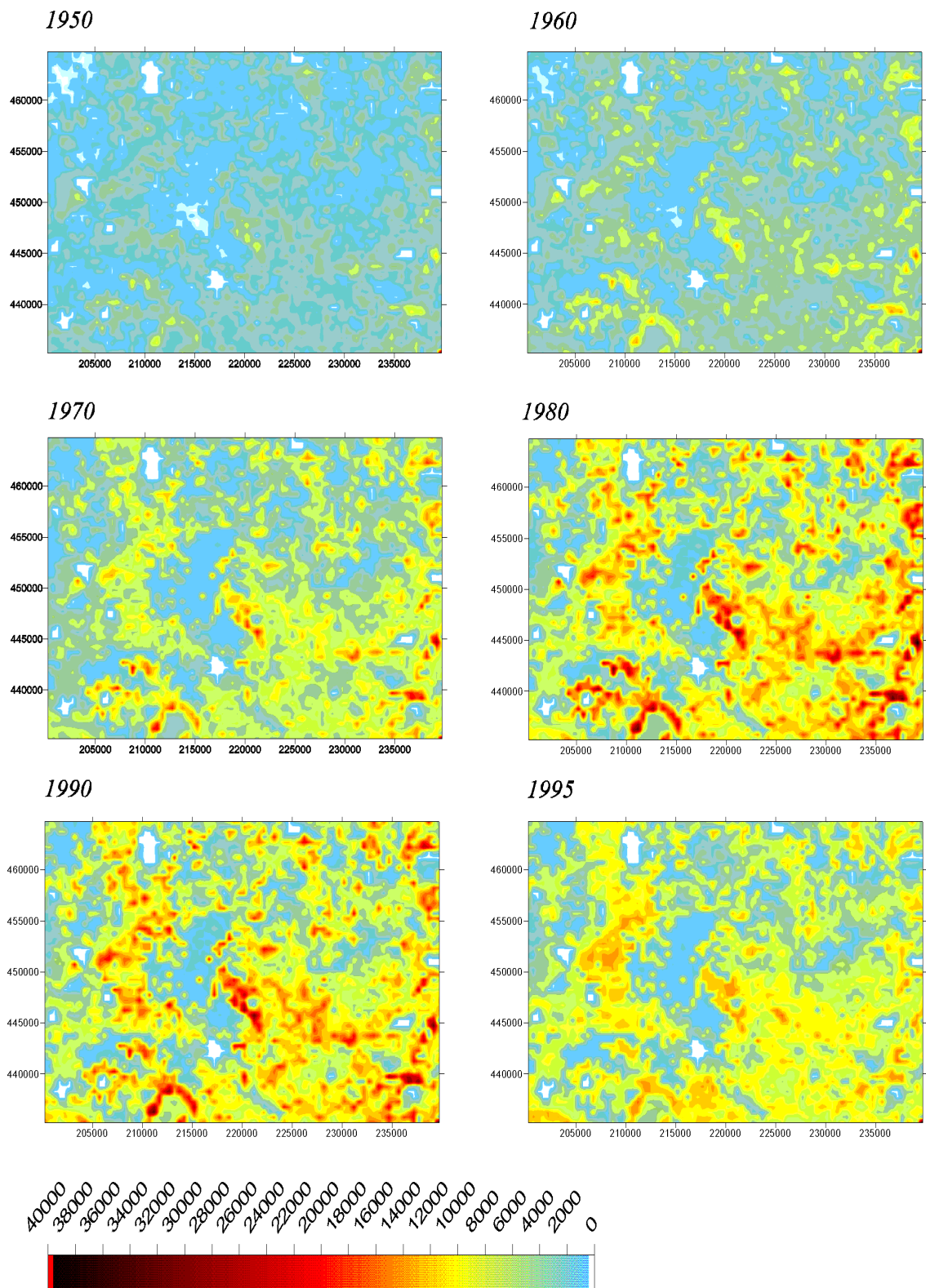
*Figure 16. Spatial distribution of nitrate flux to groundwater at several moments in time.
(Units: kg/grid-cell/year; grid cell: $500 \times 500\ m^2$) . Data by Boumans and
Van Drecht (1998).*

2.6   Nitrate Discharge in the Top System

In this section we look again at the top-system, but this time focussing on the fluxes of nitrate. The fluxes generated by the *NLOAD* program are denoted as $\Phi_{re}(x,y,t_i)$ or shortly Φ_{re}. They represent the amounts of nitrate leaching from the unsaturated zone to the groundwater (the subscript $_{re}$ indicates that these nitrates are transported by the water flux q_{re}). The transport program however, needs as top surface boundary condition the flux Φ_{as}, at least as long as this flux is downward. This boundary flux is derived below.

   With q_{re} and Φ_{re} given the nitrate concentration c_{re} can be written as:

$$c_{re} = \frac{\Phi_{re}}{q_{re}}$$

(4)

Assume that the concentrations of the water fluxes q_{as} and q_{ts} , denoted as c_{as} and c_{ts} respectively, are both equal to c_{re}. In other words, changes in the nitrate concentration during the short stay in the top system are ignored. Then, the nitrate flux into the aquifer can be written as:

$$\Phi_{as} = c_{re}q_{as}$$

or

$$\Phi_{as} = c_{re}q_{re}\frac{q_{as}}{q_{re}} = \Phi_{re}R$$

(5)

where an infiltration/discharge ratio R is introduced, defined as:

$$R = \frac{q_{as}}{q_{re}}$$

(6)

The ratio R indicates the part of the rain excess that stays in the aquifer after passage through the top system. Accordingly, the upper and lower bounds of R are considered. In case $q_{as} > q_{re}$ the entire rain excess enters the aquifer (and stays) plus an additional amount of surface water (q_{ts}) infiltrating from the drainage system. Whether the flux q_{ts} contains nitrates is not known. As a working approximation, the nitrate concentration of the infiltrating surface water is assumed to be zero. A consequence of this assumption is that Φ_{as} may not exceed Φ_{re} , so R has a maximum of 1. The other extreme of R occurs in the case of seepage. Now the discharge system removes all excess rain plus (optionally) an amount that comes from the deep aquifer system. Clearly, the nitrate flux Φ_{as} is equal to zero, so R has a minimum of zero.

   R has been calculated by (6) and plotted in Figure 17. Since q_{as} and q_{re} are both variable in space, R is a spatially distributed parameter. For areas where $q_{as} > q_{re}$, R is set equal to 1, while R is zero for $q_{as} < 0$. The ratio R indicates which fraction of the nitrate from the unsaturated zone leaches into the aquifer system. Its complement, *1-R*, indicates the fraction that is discharged
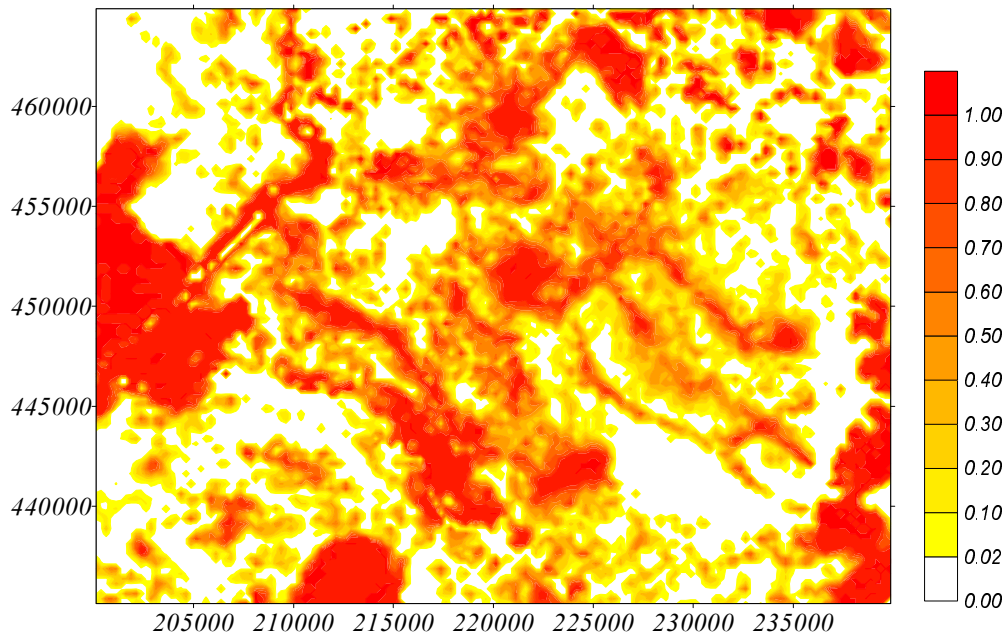
Figure 17. Spatial distribution of the infiltration/discharge ratio R.

into the top system. In Figure 17 the hilly areas of the 'Lochemerberg' in the north, 'Montferland' in the south and the foothills of the 'Veluwe' at the western boundary can be identified as typical infiltration areas (R equal or close to 1). In the white colored areas seepage occurs instead of infiltration.

The final nitrate flux into the aquifer system, Φ_{as}, follows from multiplication of Φ_{re} and R:

$$\Phi_{as} = \Phi_{re}\, R \tag{7}$$

The flux Φ_{as} as found by (7) is shown in Figure 18 .
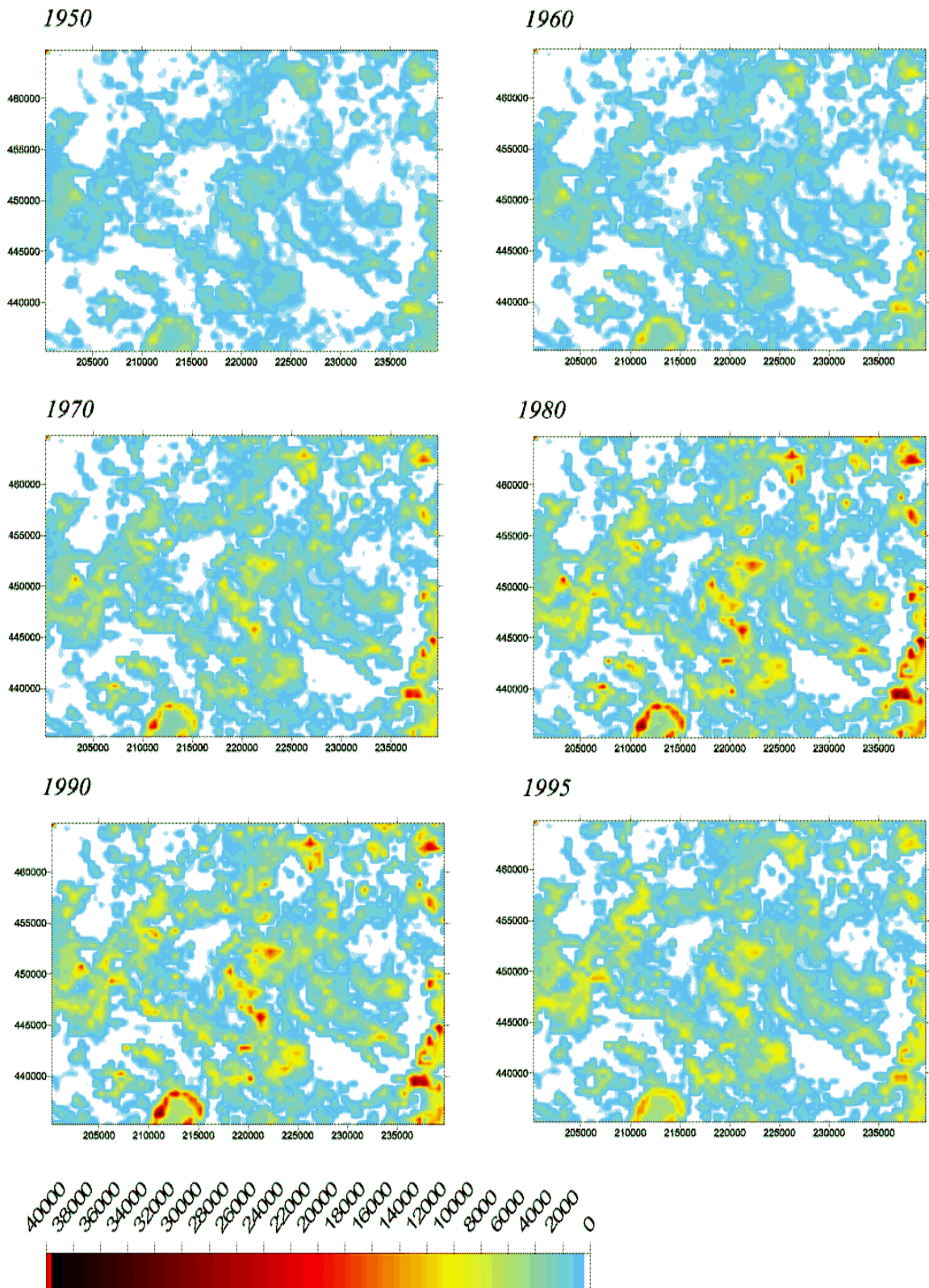
Figure 18. Nitrate fluxes Φ_{as} into the aquifer system.
   (Units: kg/grid-cell/year; grid cell: $500 \times 500\ m^2$).

2.7   Monitoring Data and other Observations

Figure 19 shows the location of the monitoring wells in the study area. For most wells three sampling depths are used ranging from 0 - 10 m, 10 - 20 m and 20 - 30 m below the surface. Appendix A gives a list with coordinates and filter-depths of the monitoring points is given, including average nitrate concentration and standard deviation for the period 1994 - 1996. For a detailed description of the Dutch Groundwater Monitoring Program see Van Duijvenbooden et al. (1985) and Snelting et al. (1990).

The total of measurements in the study area for the period 1984 - 1986 and 1994 - 1996 leads to 296 data points. Table 1 gives a general summary of the data points. In the 10 - 20 m layer no data are available for the 1984 - 1986 period.
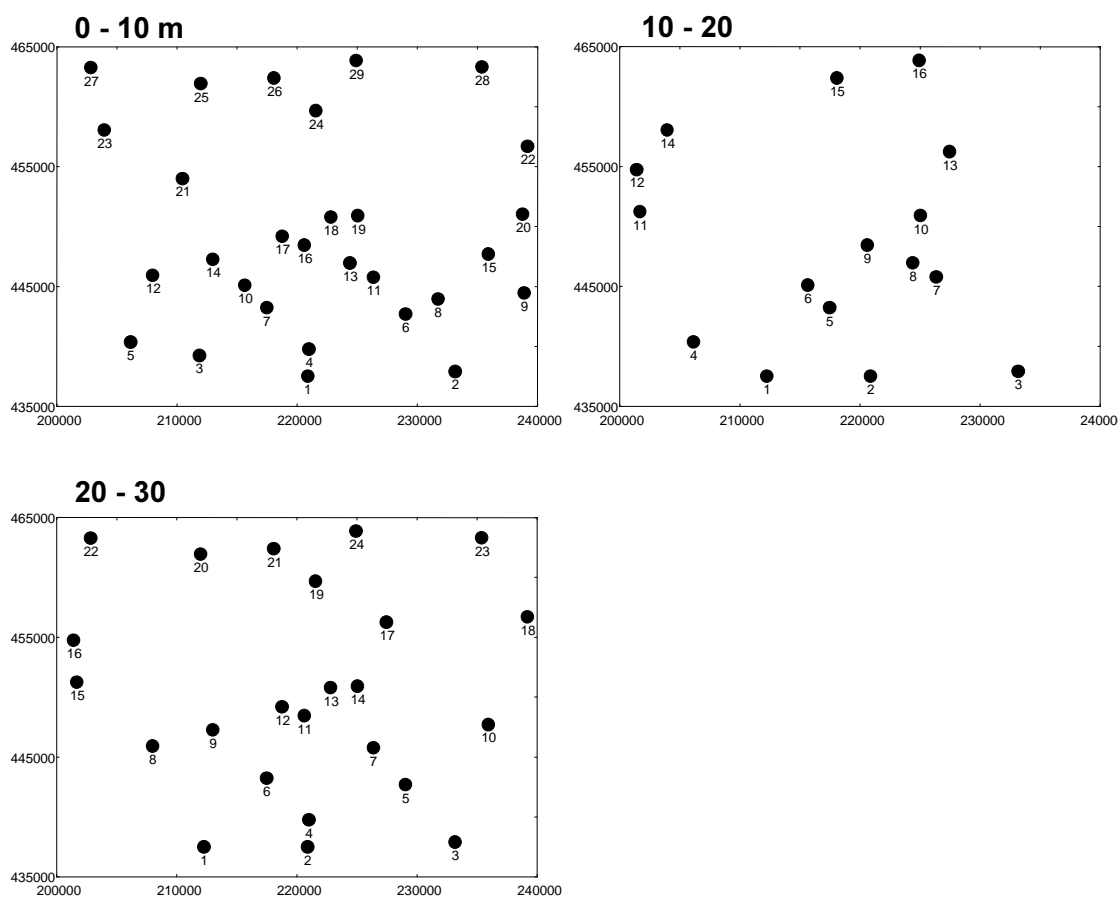
Figure 19.   Sampling locations (numbers refer to list in Appendix A).

*Table 1.   Number of observations and number of samples with
                 nitrate levels below detection limit.*

Period	Depth (m)	Total	< det.limit	% of total
1984-1986	0-10	45	24	53
	10 -20	n.p.	-	-
	20-30	45	39	87
1994-1996	0-10	95	14	15
	10-20	40	6	15
	20-30	71	14	20
Total:		296	97	33

The relation between land use, redox potential and nitrate concentrations has been investigated.
No distinction between soil types is made, since more than 98% of the samples originate from
sandy soils. Values below the detection limit are substituted by $0.5 \times$ detection-limit. Table 2
gives the average (measured) nitrate concentration broken up by categories of land use and filter-
depth. The table shows that nitrate concentrations under arable land are significantly higher (a
factor 5 - 10) than under other categories of land use. In general the concentration decreases with
depth, which may be an indication that denitrification occurs. With respect to time, a significant
increase is observed from 1985 to 1995 except for the forest area (4.4 to 2.3) in the upper 0 - 10
m layer. It is also remarkable that in most classes the range of values is large and standard
deviations often exceed the mean.

*Table 2.   Nitrate concentrations (mg NO_3 L^{-1}) in 1984-1986 and 1994-1996
              as a function of land use and depth.*

Period	Depth	Land Use			
		Urban	Forest	Arable	Pasture
1984-1986	0-10	0.12 ± 0.06	4.4 ± 3.8	32.7 ± 13.3	$0.25 \pm .034$
	20-30	0.12 ± 0.06	0.17 ± 0.13	8.1 ± 13.1	0.12 ± 0.05
1994-1996	0-10	12.7 ± 12.4	2.3 ± 3.0	49.6 ± 26.5	5.4 ± 14.5
	10-20	10.1 ± 12.9	9.2 ± 10.4	17.7 ± 22.6	0.06 ± 0.05
	20-30	0.06 ± 0.07	1.1 ± 2.1	0.5 ± 1.6	0.1 ± 0.1

In the database of the monitoring network various classes of redox-potential are distinguished ranging from oxic to sulfate reducing. A further subdivision has been made on the 1994 - 1996 data based on the redox conditions. Two classes are considered: an oxic-suboxic class representing the well to moderately well oxygenated samples ('ox'); and an iron and manganese reducing class representing the anoxic samples ('red'). The number of classes was reduced to two (in the LGM database 5 classes exist) to obtain sufficient samples in each land use type group. Table 3 gives average nitrate levels per redox class and land use type.

Table 3.   Nitrate concentrations (mg NO_3 L^{-1}) as a function of   ,
*   land use, depth and redox conditions during 1994 - 1996.*

Depth	Redox	Land Use			
		Urban	Forest	Arable	Grassland
0-10	Red	0.06 ± 0.03	0.3 ± 0.5	49.6 ± 26.5	0.04 ± 0.03
	Ox	21.1 ± 8.3	5.3 ± 2.8	49.6 ± 26.5	29.7 ± 22.1
10-20	Red	0.08 ± 0.08	0.1 ± 0.1	0.1 ± 0.2	0.06 ± 0.05
	Ox	22.7 ± 1.8	15.3 ± 9.2	32.3 ± 21.3	0.06 ± 0.05
20-30	Red	0.06 ± 0.07	0.07 ± 0.05	0.07 ±0.06	0.1 ± 0.1
	Ox	0.06 ± 0.07	3.0 ± 2.7	5.8 (n=1)	0.1 ± 0.1

Distinction in reducing and moderately oxygenated classes shows a clear contrast within each land use type group, with substantially higher nitrate concentrations in the oxic group. This is not surprising, since nitrate is reduced to nitrogen or other nitrogen compounds under reducing conditions. In the arable soil (0 - 10 m) no distinction was applied because nearly all samples fall in the oxic class. Again, this is related to the well-drained conditions prevalent within this type of land use. However, in the 10 - 20 m layer the division between oxic and reducing conditions resulted in a clear difference. Apart from the absolute levels, the degree of variation within each class is reduced substantially.

Under non-reducing conditions the highest nitrate levels are encountered in arable soils. The levels decrease in the order grassland, urban areas and forest. In general nitrate levels decrease with depth. However, high nitrate concentrations are still encountered in the 10 - 20 m layer under arable soil, urban areas and forests. In the grassland samples, nitrate levels decrease sharply with depth that is probably related to reducing conditions that prevail in most of the samples below the 0 - 10 m layer. In the samples with reducing conditions no distinction between types of land use exists.

Table 3 shows that, under reducing conditions, nitrate levels decrease drastically compared to non-reducing conditions. However, the number of data was too limited to prepare meaningful maps of redox conditions. Attempts to produce these maps have resulted in non-realistic representations (maps not shown here). The percentages of samples with (sub)oxic conditions decrease with depth respectively from 53 % and 46 % in the 0 - 10 m and 10 - 20 m layer to 8 %

in the 20 - 30 m layer. This indicates that in the 20 - 30 m layer reducing conditions prevail throughout the study area. However, in the upper two layers, redox conditions vary considerably throughout the area. This has a profound effect on the spatial variability of nitrate concentrations in the upper groundwater (in this case the layer between 0 and 20 m below the surface). Summarizing the discussion above leads to the following:

- Nitrate levels are related to land use (i.e. positively correlated with nitrogen load) and are highest in arable land and lowest in forest soils.
- Under reducing conditions, nitrate levels are strongly reduced (< 1 mg L^{-1}) and are similar in all land use types.
- In the upper two layers, spatial variability in redox conditions is most likely one of the key parameters in determining spatial variability in nitrate concentrations (together with land use and/or nitrogen load).

3   MODEL DESCRIPTION AND SIMULATION RESULTS

3.1   LGMCAD

Particle Tracking

The solute transport model LGMCAD is based on a so-called Lagrangian approach. This means that point masses (particles) are introduced that carry a certain, possibly varying, amount of solute mass and accordingly, the displacement of the particles is calculated by solving the particle motion equations. This technique is known as *particle tracking*. The Lagrangian approach is consistent with Eulerian approaches such as the Finite Element Method. Its main advantage is that during calculation complications as numerical dispersion are more easily controlled. Several numerical test have been carried out to compare LGMCAD with known analytical solutions with satisfying results (Uffink, 1996). The main process that causes solute displacement is the flow of groundwater itself. When the $\vec{v} = (v_x, v_y, v_z)$ denotes the groundwater velocity vector, where v_x, v_y and v_z are the components along the x, y and z coordinate axis respectively, then we can write for the displacement during a time interval Δt :

$$\begin{aligned} \Delta x &= v_x \Delta t \\ \Delta y &= v_y \Delta t \\ \Delta z &= v_z \Delta t \end{aligned} \qquad (8)$$

The displacement due to the groundwater flow is called the advective displacement.

Random Walk

Particle tracking as described above can be extended with additional term that take into account mixing by dispersion. This method is known as the Random Walk Method (Uffink, 1990). The method starts by generating three mutually independent numbers, denoted here by R_i (with $i = 1, 2, 3$). The numbers are generated such that:

$$E\left[R_i R_j\right] = 0 \text{ for } i \neq j$$

and   (9)

$$E\left[R_i R_j\right] = 1 \text{ for } i = j.$$

(*E[x]* stands for the expectation of *x*).

The total particle displacement now can be written as:

$$\Delta x = v_x \Delta t + a_{11} R_1 + a_{12} R_2 + a_{13} R_3$$

$$\Delta y = v_y \Delta t + a_{21} R_1 + a_{22} R_2 + a_{23} R_3 \tag{10}$$

$$\Delta z = v_z \Delta t + a_{31} R_1 + a_{32} R_2 + a_{33} R_3$$

The components a_{ij} are given by:

$$a_{11} = \frac{v_x}{|v|}\sqrt{2\alpha_L |v| \Delta t} \ , \qquad a_{12} = -\frac{v_y}{\sqrt{v_x^2 + v_y^2}}\sqrt{2\alpha_T |v| \Delta t} \ , \qquad a_{13} = -\frac{v_x v_z}{|v|\sqrt{v_x^2 + v_y^2}}\sqrt{2\alpha_T |v| \Delta t} \ ,$$

$$a_{21} = \frac{v_y}{|v|}\sqrt{2\alpha_L |v| \Delta t} \ , \qquad a_{22} = \frac{v_x}{\sqrt{v_x^2 + v_y^2}}\sqrt{2\alpha_T |v| \Delta t} \ , \qquad a_{23} = -\frac{v_y v_z}{|v|\sqrt{v_x^2 + v_y^2}}\sqrt{2\alpha_T |v| \Delta t} \ ,$$

$$a_{31} = \frac{v_z}{|v|}\sqrt{2\alpha_L |v| \Delta t} \ , \qquad\qquad a_{32} = 0 \ , \qquad\qquad a_{33} = \frac{\sqrt{v_x^2 + v_y^2}}{|v|}\sqrt{2\alpha_T |v| \Delta t} \ ,$$

$$\tag{11}$$

where $|v| = \sqrt{v_x^2 + v_y^2 + v_z^2}$ and α_L and α_T denote the longitudinal and transversal dispersivity.

Details on the theoretical background of the random walk are found in Uffink (1990), while the implementation of the method in LGMCAD is described in Uffink (1996). A User's manual for LGMCAD is available (Uffink, 1999).

3.2   Data Processing

Grids
Since LGMCAD is a particle model, the principal output is a list of particle coordinates and particle masses. For the conversion of these data to nitrate concentrations a program CLDGRID is available (Uffink, 1999). Concentrations obtained with CLDGRID are spatially structured on a *grid* that is regularly distributed in horizontal directions. For various moments in time concentration grids can be obtained. A grid may have a variable elevation and thickness and looks like a 'slice' cut out of the aquifer system (Figure 20).

From the concentration grids contour maps are obtained with the program SURFER. Throughout the study grids with a horizontal resolution of 500×500 m^2 are applied. With this resolution the grids consist of 80×60 cells.
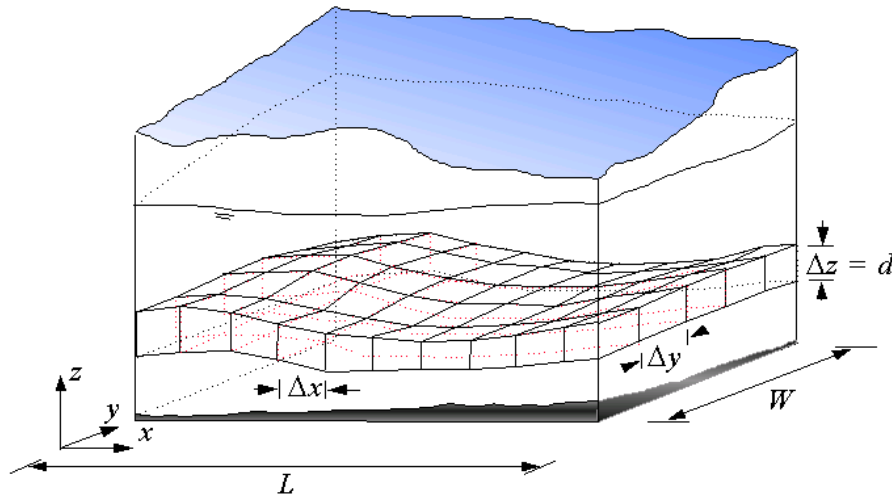
Figure 20.   'Grid' with varying elevation and thickness d.

Three grids with a constant thickness of 10 meters have been defined at different vertical positions. Grid-1 is located between the phreatic surface and 10 m *below* this surface. Grid-2 ranges from 10 m to 20 m and Grid-3 from 20 m - 30 m below the phreatic surface.

Individual cells (monitoring cells)
Apart from concentrations on a structured two-dimensional grid, output data can be converted to concentrations in individual cells. Such a cell, referred to as 'monitoring cell', may be located at any given depth of the aquifer. For the processing of the output data 'monitoring cells' have been chosen at locations that coincide with the filters of the monitoring wells.

3.3   Preliminary Results

For a first impression of the systems behavior several preliminary runs have been executed with standard settings. Detailed information on the input files for some runs can be found in Appendix B. No denitrification has been considered in the first (preliminary) run. Figure 21 shows the concentrations in the year 1995 for the three selected depths (grid structured data). We refer to these layers as *top layer* (0 - 10 m), *middle layer* (10 - 20 m) and *bottom layer* (20 - 30 m). All depths are with respect to the groundwater surface. The line A-B in Figure 21b indicates the position of a cross-section shown in Figure 22.
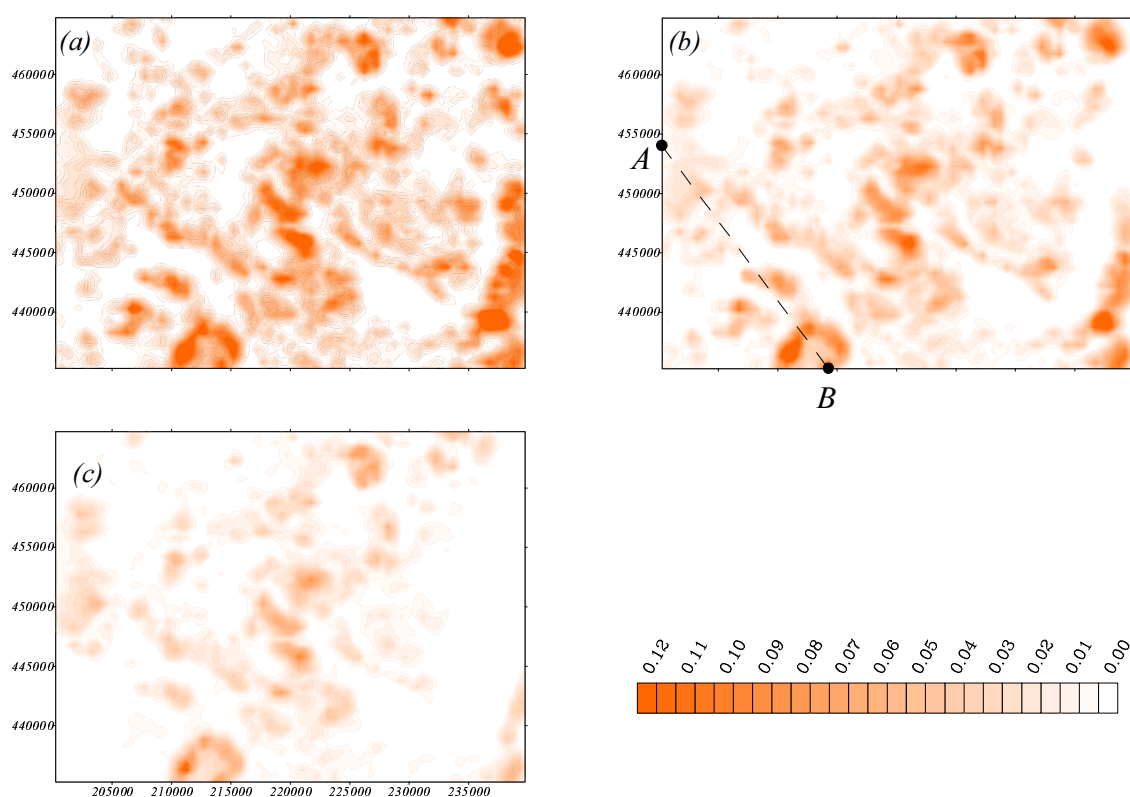
Figure 21.   *Modeled nitrate concentration (in g L^{-1}) in 1995 without decay.*
             Depth (a) 0-10 m; (b) 10-20 m; (c) 20-30 m.

In the top layer several regions with high nitrate levels can be seen, mostly located in the central part of the study area where intensive animal husbandry is common. In the western section nitrate levels are lower due to land use, soil type and hydrologic conditions. Especially in the hilly area at the western border (Veluwe) the average *N*-load is low. In the IJssel valley poorly drained clay soils prevail with high groundwater levels. At most places along the eastern boundary the aquifer thickness is around 20 m or less, which explains why in the layer between

20-30 meter (Figure 21 c) along most of the eastern boundary no data are present. At the Veluwe hills high infiltration rates occur in combination with a low N-load. The situation is different in 'Montferland', where infiltration is combined with relatively high leaching rates.

In general, nitrate levels are decreasing with depth, partly because at greater depth the water is of older age and during the 50's and the 60's water has infiltrated with substantially lower nitrate contents than during the 90's. Another explanation is the occurrence of mixing by dispersion. As can be seen from Figure 21, high deposition in the 'hot-spots' still affects the groundwater down to the bottom layer. Comparison of the three layers suggests that the horizontal displacement is of minor importance: areas with high nitrate levels seem to remain at its place. However, this is a matter of scale. Regionally the horizontal displacement in 45 years is not very significant, but on local scale things may be different.

The influence of the hydrology is more clearly seen in a vertical cross section (Figure 22).
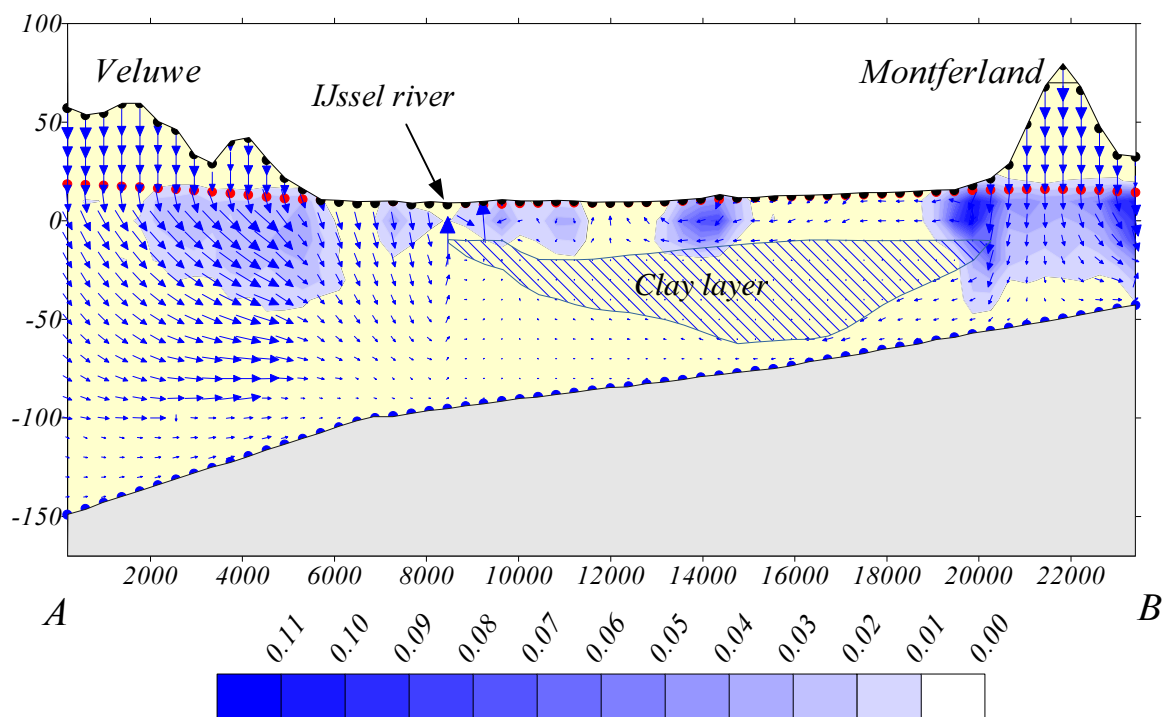
Figure 22.   Calculated nitrate concentration in saturated zone (in g L^{-1}) in 1995 in vertical cross-section A - B. Vertical: Depth in meter NAP. Horizontal: Distance from A to B in meters. Red dots indicate the phreatic surface.

The section was chosen that cuts across two infiltrating areas and a seepage area, i.e. starting at the Veluwe foot-hills running across the IJssel valley towards the hills of Montferland. The location is indicated in Figure 21 (b) as the line *A-B*. Under and around the hills of Montferland high nitrate concentrations occur, while the nitrate pollution is moderate at the edge of the Veluwe. Between the infiltration areas a region with a relatively low groundwater velocity occurs, due to the presence of a thick clay layer (Drenthe clay; see Figure 5). At the right hand side the plume of nitrate tends to split in a part that moves underneath the clay layer and another that stays above. The red dotted line indicates the location of the phreatic surface. The unsaturated zone, located above the red dotted line shows no nitrate, since the model data only refer to the saturated zone. Obviously, nitrate pollution also occurs in the unsaturated zone, since the nitrate comes from the land surface.

3.4   Denitrification

In a second set of runs denitrification was simulated by a first order decay process:

$$c(t) = c_0 \exp(-\lambda t) \tag{12}$$

where c_0 denotes the initial concentration and λ is the decay rate $[\text{T}^{-1}]$. Instead of λ, the rate of decay is often expressed by the half-life time, denoted as T_{50}. The relation between λ and T_{50} is:

$$T_{50} = \frac{\ln(2)}{\lambda} \tag{13}$$

In order to compare the effect of half-life time on model results, several runs have been executed with different values for T_{50}. At first, we have used a single decay rate for the whole area. In Table 4 the average concentration for each of the selected layers is given for the year 1995. It is clearly seen that nitrate levels decrease as T_{50} decreases. Figure 23 shows the effect of the increased decay rate on the nitrate concentrations for the top and the bottom layer.

Table 4 Effect of decay rate on model predictions
(Average Nitrate Concentrations in mg NO$_3$/L)

T_{50}		Top	Middle	Bottom
2	(year)⁻	5.7	1.2	0.2
5	(year)	10.2	3.6	1.0
10	(year)	14.9	7.1	2.7

Top layer

Bottom layer

$T_{50} \, \infty$

$T_{50} = 10 \, yr$

$T_{50} = 2 \, yr$

time: 14500 days
depth: 0 - 10 m (a), (c), (e)
20- 30 m (b), (d), (f)

0.12 0.11 0.10 0.09 0.08 0.07 0.06 0.05 0.04 0.03 0.02 0.01 0.00
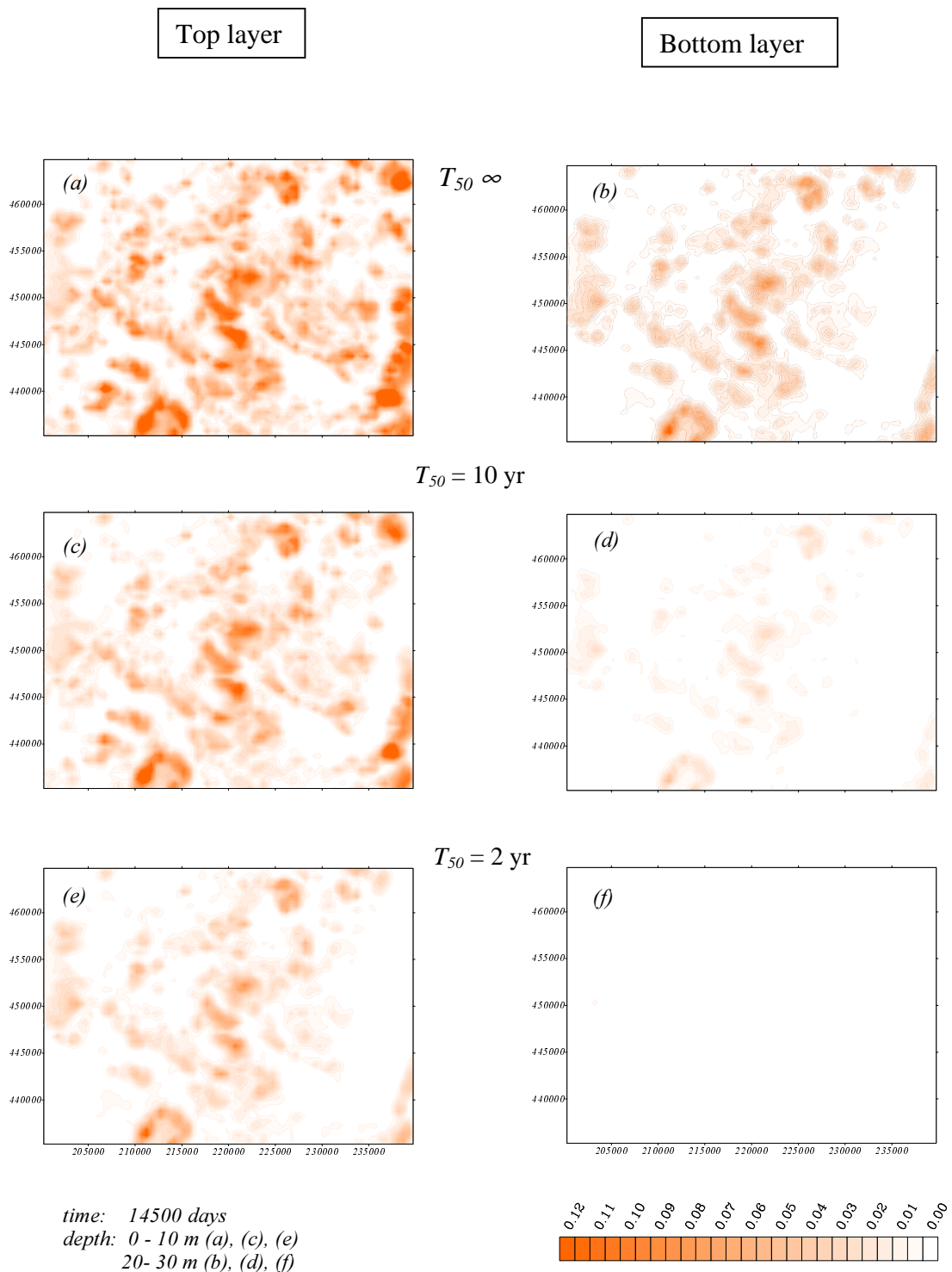
*Figure 23.   Effect of decay rate on nitrate distribution in 1995 for various decay rates
(Concentration in g L^{-1}). No denitrification ($T_{50} = \infty$) for (a) and (b),
T_{50} is 10 years for (c) and (d); T_{50} is 2 years for (e) and (f).*

3.5   Model Refinement and Final Results

For a detailed evaluation of the simulations we introduce E_1, a figure that indicates how well a run 'scores' with respect to the measured data. In fact, E_1 represents an object function that needs to be minimized. E_1 is defined below. First, the concentrations, both measured and calculated, are log-transformed. Since the order of magnitude of the concentrations varies widely, it makes more sense to consider concentration ratios (or differences of the logarithms of the concentrations) than concentration differences:

$$Y_i^m = \ln c_i^m \tag{14}$$

$$Y_i^c = \ln c_i^c \tag{15}$$

Here c_i^m is the measured concentration and c_i^c the calculated concentration at an individual measuring point i. The calculated concentration refers to the concentration in a so-called 'monitoring' cell. The centers of these cells coincide with the coordinates of the filters of monitoring wells. The dimensions of the cells are 100×100 m^2 horizontally and 10 m vertically. The calculated concentration is representative for a volume of $100 \times 100 \times 10$ m^3, which is considerably larger than the volume of the measuring samples. When smaller monitor cells are chosen, the results will contain a higher level of statistical noise and may become meaningless. After the log-transformation the differences between calculations and measurements (residuals) are squared and summed:

$$E_1 = \sum_{i=1}^{N} \left(Y_i^m - Y_i^c \right)^2 , \tag{16}$$

where N is the number of locations. E_1 is a dimensionless number, which is clear since the residual $Y_i^m - Y_i^c$ is equal to $\ln\left(c_i^m / c_i^c \right)$. The calculated data refer to the situation after 45 years since the start of the simulation. This is supposed to represent the year 1995. The 'measurements' are collected between 1994 and 1996 (see appendix A). Table 5 gives E_1 for various runs for the total model area as well as for the layers separately. It appears that without denitrification ($T_{50} \rightarrow \infty$) predicted nitrate levels are excessively high. Including decay improves the fit of the data. For the middle and bottom layer a good fit occurs for $T_{50} = 1$ year. In the top layer the best fit is obtained for $T_{50} = 5$ years. A faster decay rate worsens the fit in the top layer, although the overall fit (see total) improves.

Table 5 E_1 for various decay parameters

T_{50}	unit	Total	Top	Middle	Bottom
1	(year)	584	378	174	32
2	(year)⁻	493	268	183	43
5	(year)	549	231	199	118
10	(year)	595	206	198	191
∞	(no-decay)	880	254	282	344
Number of Data		69	29	16	24

A second indicator for the match of the data is the sum of the residuals of the log-transformed concentrations:

$$E_2 = \sum_{i=1}^{N} \ln \frac{c_i^{m}}{c_i^{c}} \quad = \sum_{i=1}^{N} Y_i^{m} - Y_i^{c} \tag{17}$$

This figure indicates whether the average level of the calculated concentration is above or below the level of the measurements. When E_2 is positive, measurements are (on the average) higher than the calculated data and vice versa. Note that E_2 is a dimensionless number.

Table 6 E_2 for various decay parameters

T_{50}	unit	Total	Top	Middle	Bottom
1	(year)	77	44	18	14
2	(year)	25	22	4	-1
5	(year)	-39	-5	-8	-26
10	(year)	-86	-17	-26	-43
∞	(no-decay)	-140	-39	-38	-63

Tables 5 and 6 suggest that a decay rate between 1 and 2 years is reasonable for the deeper layers (middle and bottom), but for the upper layer this value produces nitrate concentrations that are too low. $T_{50} = 5$ - 10 year gives a good fit in the upper layer, but now too much nitrate is found in the deep layers. For this mismatch several explanations are possible:
i)   The model produces too much mixing in vertical direction.
ii)   The model overestimates advective transport in vertical direction.
iii) Degradation rates at greater depth are too low.

Each of the explanations mentioned above suggests a modification of the model. Below these modifications are briefly discussed.

ad i)

Some evidence exists that the model overestimates vertical dispersion. This may be explained by considering the following two situations. The first concerns purely *horizontal* flow. Here the transverse dispersion has both a horizontal and a vertical component. The model applies only one value for the transverse dispersivity (α_T = 1 meter), i.e. the same value for the vertical and the horizontal direction. It has been reported (Rajaram and Gelhar, 1991), that vertical transverse dispersion can be extremely small and even may be in the order of magnitude of molecular diffusion. Field studies (Maas, 1984; Uffink, 1990) have confirmed that such low values also occur in Dutch sand formations. Thus, without distinction between vertical and horizontal transverse dispersion, the model may easily overestimate the vertical mixing.

The second situation we consider is that of purely *vertical* flow. Although purely vertical flow is not often encountered in deep aquifers, the vertical flow component can still be significant at or near infiltration sites. In the case of purely vertical flow longitudinal dispersion is responsible for the vertical mixing. Again, the model utilizes only one value for longitudinal dispersivity (α_L). This value is applied both for horizontal and vertical flows (and everything in between). In the present study α_L is assumed to be 10 meter, which is a reasonable value for horizontal flow. However, for vertical flow or almost vertical flow it leads to a mixing that is unrealistically high. One of the advantages of the particle concept of the transport model is that extremely low dispersivities values (even zero) may easily be applied, without suffering from artificial numerical mixing (numerical dispersion). In the following runs dispersion in vertical direction has been switched off, i.e. reduced to the level of molecular diffusion. In horizontal direction the original concept of dispersion is preserved.

ad ii)

The advective solute flux follows directly from the groundwater flow. However, the vertical and horizontal flow components are obtained by essentially different techniques. The *horizontal* velocity is derived by differentiation of the head-distribution and subsequent application of Darcy's law, where the hydraulic conductivity (permeability) indicates how much water flows at a given head gradient. In the *vertical* direction no head gradients are determined. The model applies the Dupuit-Forchheimer assumption, which means that within an aquifer the head is assumed constant over the vertical. The vertical flow component is obtained from the continuity equation by a procedure described by Strack (1984). It can be shown that these results are similar as when an infinitely high vertical permeability is assumed. This means that in the model no resistance to vertical flow occurs. In reality always some resistance to vertical flow exists, so the Dupuit-Forchheimer model leads to an overestimated advective transport in vertical direction. In the next set of runs we have introduced a slightly modified vertical distribution for the vertical flow component as a compensation for the overestimation. Details are described in an appendix C.

ad iii)

The low nitrate concentrations found in the deeper layer are difficult to match by model results using a constant decay parameter throughout the domain. The data rather suggest that the denitrification capacity increases with depth. Meinardi (1999) has stated that e.g. in the aquifer near Hupsel denitrification occurs due to contact between the deep groundwater and the clay layers at the base of the aquifer. Also in other parts of the area clay-layers are present that are expected to have the same nitrate reducing capacity. Therefore, for the next set of runs a spatially varying decay parameter is applied according to the following scheme (see Figure 24).
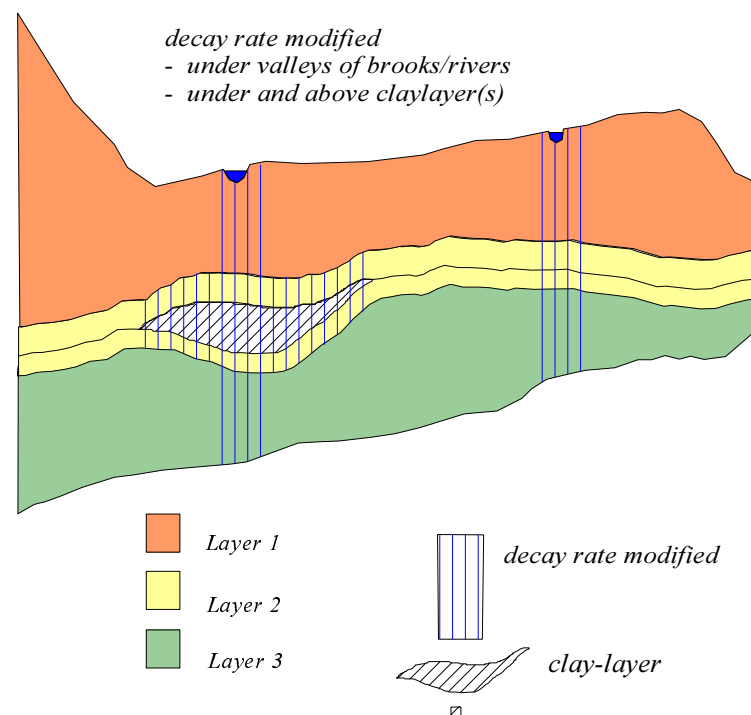
Figure 24. Vertical scheme for distribution of decay parameter.

First, a constant background decay parameter (e.g. $T_{50} = 5$ year) is assigned to the entire study area. This parameter is overwritten in areas where higher decay rates are likely. Higher decay rates are expected, for instance, close to clay layers. Figures 5 and 6 (Chapter 2) show the extensions of two regional clay-layers. We consider only the more important of the two layers, i.e. the Drenthe clay. A modified decay rate (e.g. $T_{50} = 2$ year) is applied in a zone of 5 m above and below the clay-layer including the clay itself. The nitrate reducing capacity is expected to be high also in the neighborhood of local clay and peat-layers underneath river-valleys. The spatial distribution of the decay parameter as described above has been implemented in the model in the following way (Figure 24). Throughout the model area three horizontal layers have been defined. The first (layer 1) extends vertically from the top of the aquifer system (land surface) to 5 meters above the top of the clay layer (if present). In this layer the decay parameter is

overwritten only underneath the valleys of brooks and rivers. Layer 2 extends vertically from 5
meters above the clay to 5 meters below. It includes the clay layer entirely. Where the clay-layer
is absent the thickness of layer 2 is exactly 10 meter while its elevation is more or less arbitrary.
The decay parameter is overwritten underneath valleys of rivers and brooks and above,
underneath and inside the clay-layer. The third layer (layer 3) extends from the bottom of layer 2
to the base of the aquifer system. The distribution of the decay parameter is the same as in layer
1. The Figures 25 and 26 present the horizontal distribution of the decay parameter for the
different layers.
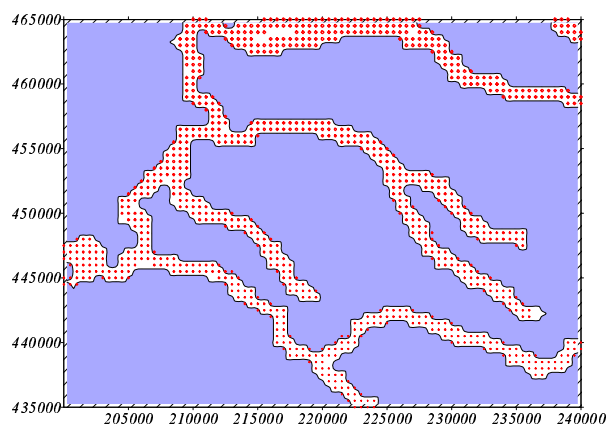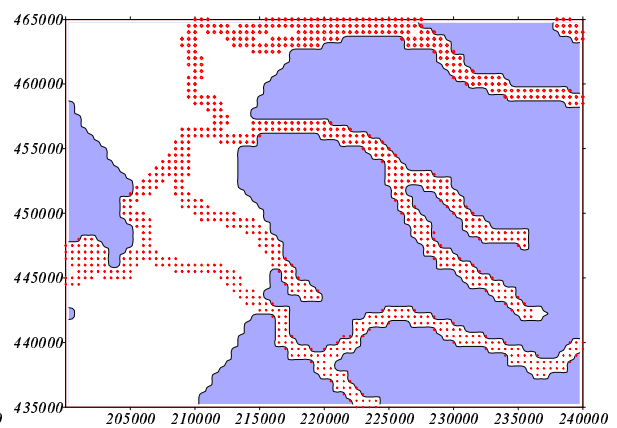
Figure 25   *Figure 26*

Figure 25. Decay rates in layer 1 and layer 3. Blue: back ground value (T_{50} = 5 years);
White + red dots: valleys of rivers and brooks (T_{50} = 2 years).

Figure 26. Decay rates in layer 2. Blue: back ground value (T_{50} = 5 years);
White: Presence of clay layer (T_{50} = 2 years).
White + red dots: valleys of rivers and brooks (T_{50} = 2 years).

Results of Refined Model

Table 7 gives the figure E_1 for a series of runs with the following characteristics:

Case 5a: T_{50} is 5 years; no further refinement. Identical to preliminary runs.

Case 5b: For T_{50} a background value of 5 years is applied, while $T_{50} = 2$ years in valleys of brooks and rivers, in the Drenthe clay and in a zone of 5 meters above and below this clay layer.

Case 5c: As case 5a, but with vertical dispersion switched off (diffusion only).

Case 5d: As case 5a, but the distribution of the vertical flow component (Dupuit-Forchheimer) modified.

Case 5e: As case 5a, but vertical dispersion switched off and the Dupuit-Forchheimer assumption modified ($\gamma = 0.5$).

Case 5f: As case 5b, but vertical dispersion switched off, and the Dupuit-Forchheimer assumption modified.

All data in Table 7 and 8 refer to the situation at $t = 1995$.

Table 7   *E_1 for various runs*

Case	T_{50}	Vertical Dispersion	DF Modified	Total	Top	Middle	Bottom
5a	Constant	On	No	549	231	199	118
5b	Variable	On	No	478	171	185	122
5c	Constant	Off	No	392	163	182	46
5d	Constant	On	Yes	456	141	184	129
5e	Constant	Off	Yes	396	161	186	48
5f	Variable	Off	Yes	389	150	188	52

From Table 7 it appears that the difference between a constant and a spatially variable decay parameter is not striking. Moreover, the difference is not systematic. Comparison of the cases 5a and 5b shows an improved fit in the top layer, but the fit is worse for the middle and bottom layer. With other modifications implemented (vertical dispersion off and Dupuit-Forchheimer modified; see cases 5e and 5f) spatial variation has only little effect, while the overall 'score' is slightly worse than with a constant parameter. The most dramatic change is obtained when vertical dispersion is switched off (5a versus 5c; 5d versus 5e). Finally a series of the runs with different half-life time is summarized in Table 8.

Table 8 E_1 for various runs with different half-life times

Case	T_{50}	Vertical Dispersion	DF Modified	Total	Top	Middle	Bottom
2e	*Constant*	*Off*	*Yes*	434	250	153	32
3e	*Constant*	*Off*	*Yes*	369	189	157	23
4e	*Constant*	*Off*	*Yes*	362	159	168	34
5e	*Constant*	*Off*	*Yes*	396	161	186	48
6e	*Constant*	*Off*	*Yes*	408	155	195	57

4   DISCUSSION

Spatial variation of decay parameter
In the previous chapter a scheme has been proposed for the spatial variation of the decay parameter. This scheme was inspired by the information that close to the separating clay-layers and underneath the rivers and brooks organic material is present, which increases the denitrification capacity. However, the difference between the model results based on a constant decay and those with a spatially variable parameter is not great. The reason may be that most monitoring wells are outside the zone where the decay parameters have been modified. Figure 27a shows the location of the monitoring wells with filters in the top layer (0 - 10 m) together with the location of river-valleys and brooks. In the white colored areas the decay rate has been increased. The Figures 27b and 27c show the wells with filters in the middle and bottom layer. The background map also shows the presence of the clay-layer. Most of the wells are clearly outside the areas where T_{50} is adjusted.

(a)

(b)   (c)
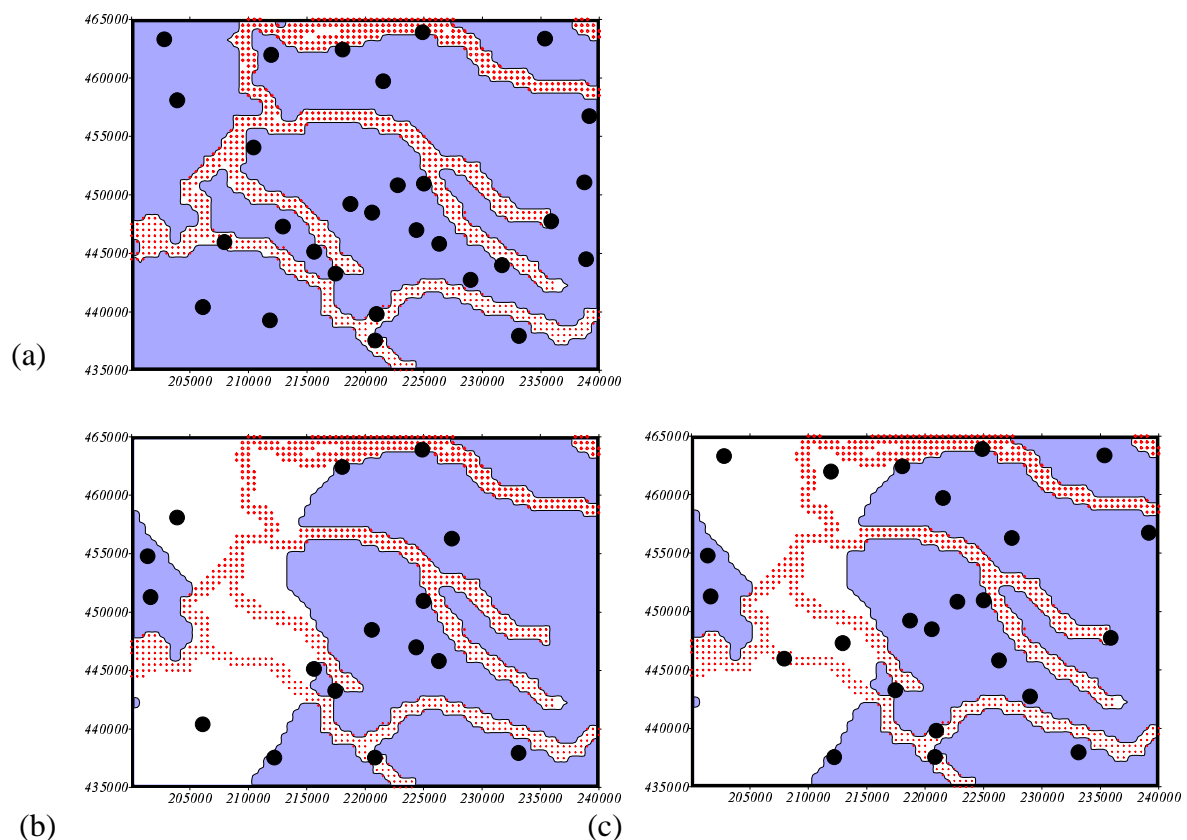
Figure 27. Location of monitoring wells with respect to spatial variation of decay parameter.
(a)   upper layer with decay parameter modified in the valleys of rivers and brooks.
(b)   middle layer with decay parameter modified in the valleys of rivers and brooks and near the clay layer.
(c)   bottom layer with decay parameter as in (b).

In the present study the rate of denitrification has only been related to the occurrence of organic matter as far as this can be expected from the presence of rivers and other streams of the existence of regional clay layers. In principle the decay parameter may be correlated to other parameters. For instance, it is known that nitrate levels can also be reduced by oxidation of pyrite (Appelo and Postma, 1993). An indication for this mechanism is the simultaneous increase of sulfate and iron with the decrease of nitrate. Several cases have been reported in the literature.

Variability and Representativeness
Figure 28 shows for each individual monitoring point the parameter E_2. This parameter denotes the difference between (log-transformed) observed and calculated concentrations also known as the residual. The data refer to the case 5c from Table 7 and the situation at $t =1995$. The data are grouped for the depth of the monitoring screen (left figure) and for land use (right figure). Often, the individual residuals can reveal some important features of the model fit. Two striking points can be noticed here. According to the figure at the left-hand side the variability in the bottom layer seems lower than in the other layers. A possible explanation may be that the variations are due to seasonal changes or other climatic variations in time. Such variations decrease and level out at greater depth. The figure at the right hand side suggests that under urban areas the difference is systematically greater than zero, which means that the measured data are higher than the calculated ones. The data for forest areas are biased to the negative side, although less pronounced than in the case of urban data. The data on the release of nitrate, as generated by *NLOAD*, may be responsible for the bias. Otherwise, it indicates that higher or lower denitrification rates must be applied under, respectively, forest and urban areas.
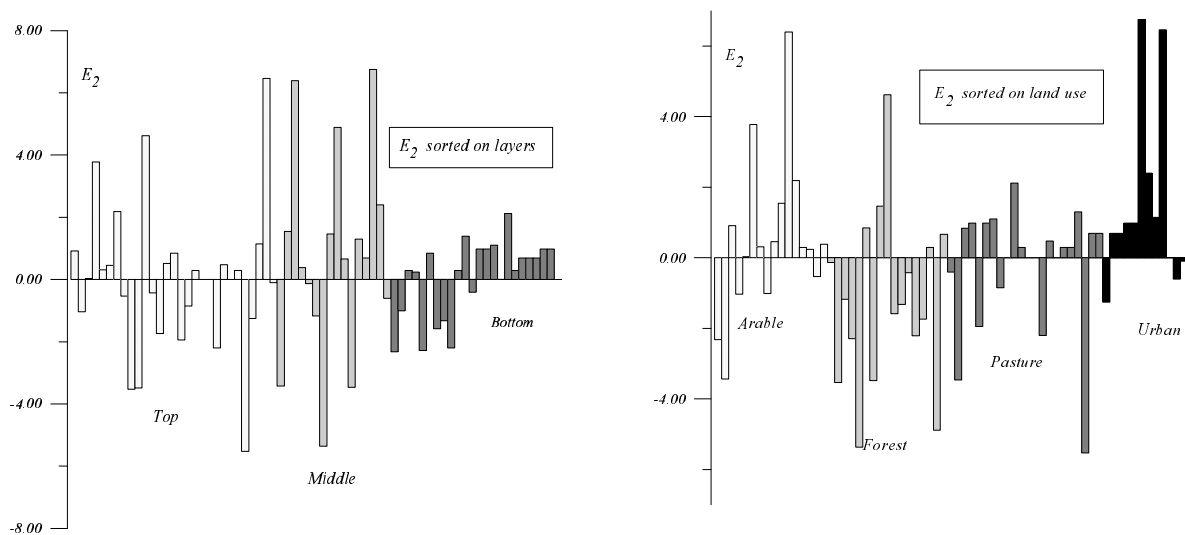
Figure 28. Residuals of log-transformed concentrations for individual monitoring points grouped for screen depth (left) and type of land use (right).

Several aspects concerning the representativeness of the monitoring data and the simulation results must be taken into consideration. First, the measured concentrations are local values with a small representative volume. In the sampling procedure a volume of approximately 5 liters of water is extracted and the representative volume is in the same order of magnitude. The simulated concentrations are determined for a volume with horizontal dimensions of 100×100 m^2 and a thickness of 10 m. Clearly, this volume is considerably larger than that of the measuring samples. Secondly, the measurements vary in time due to seasonal variations and other annual variation in the climate. E.g., the measurements may reflect whether the year of infiltration was typically dry or wet. The simulation, however, is based on a 'standard hydrologic year' and seasonal or climatological changes are not taken into account.

In addition, there is an effect of the discretization of solute mass. The diffuse and continuous concentration is modeled by a distribution of a finite number of point masses (particles). The discretization effect depends mainly on two decisions by the user of the model. The first, taken prior to the calculation, concerns the number of injected particles. The greater the number of particles, the better the resolution of the concentration distribution but the longer the runtime. Besides, for practical purposes an upper limit exists for the total number of particles that can be tracked simultaneously. In the present model version the limit is 10^6 particles. The second decision is taken during post-processing and concerns the size of the monitoring cell. Such a cell is required to convert the particle distribution to a solute concentration. Here, the trade-off is between resolution and statistical noise. A cell must be large enough to 'catch' a sufficient number of particles; otherwise the presence of particles in the cell becomes a pure matter of chance. However, a larger cell means less resolution. At present no guidelines exist for an optimal choice of cell size and number of injected particles. Satisfactory values must be found by trial and error. Below, details for the present simulations are described with some comments.

The release rate of nitrates, which is a continuous flux, is modeled by a number of discrete pulses (N_{pulses}). At each pulse a number of particles (N_{ppp}) is released. The model-user chooses i) the number of particles per pulse N_{ppp} ii) the time interval between the pulses and, indirectly, the number of pulses N_{pulses}. The total number of injected particles becomes: $N_{p\_tot} = N_{ppp} \times N_{pulses}$. For the present study we have applied a pulse interval of 180 days over a total run-time of 16400 days (simulation period 1950-1995), resulting in approximately 91 pulses ($N_{pulses} = 91$). With an upper limit for N_{p_tot} of 10^6 the maximum number of particles per pulse becomes $N_{ppp} = 11,000$. In practice N_{ppp} may be chosen somewhat higher, since not all particles will be active in the aquifer system simultaneously. Part of the first injected particles have left the aquifer before the last ones are injected. In our simulations we applied an average number of 12,000 particles per pulse resulting in a run-time of 6-10 hours on a HP Apollo workstation. At the end of the simulation period the total number of particles was approximately 600,000. As the total volume of infiltrated water is 3.4×10^5 m^3/day, it appears that - on the average - one injected particle represents the solute mass that is contained in a groundwater volume of $180 \times 3.4 \times 10^5$ /12000 = 5,100 m^3. Then, the expected number of particles in the monitoring cell will be $n \times V_{mon\_cell}$ /5,100 = 5.9 , where $V_{mon\_cell} = 10^5$ m^3. In the present study we have experimented with a

refinement of the pulse distribution in time, i.e. a shorter pulse interval at the end of the run-time when release rates are higher. A further reduction of the noise is possible by refinement of the particle distribution in space, e.g. close to the monitoring wells. However, the present version of the model does not have this option.

Figure 29a presents the number of particles found in each monitoring cell at $t = 1995$, while the figure below (29b) shows the residual log-concentrations. It is seen that the three largest 'outliers' are based on very few particles (1 or zero). Therefore, they contain a high level of statistical noise and must be considered to be unreliable.

(a)

(b)
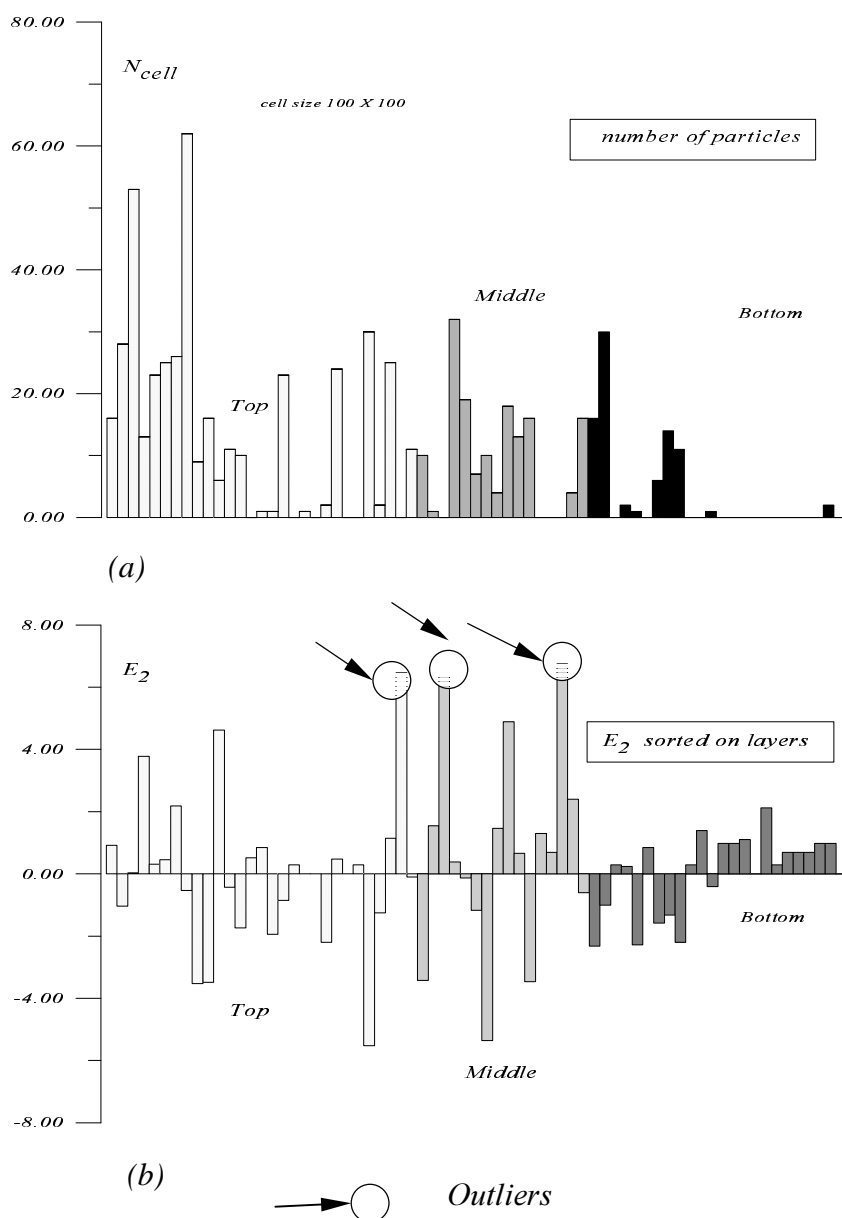
Figure 29. (a) Number of particles found in each monitoring cell. Cell size $100 \times 100 \times 10$.
(b) Residuals of log-transformed concentrations for individual monitoring points.

Size of monitoring cell

Several runs have been reevaluated with using monitoring cells of $250 \times 250 \times 10$ m^3. The results are presented in Figure 30. The number of particles found in the cells is considerably higher, but the 'outliers' are still supported only by one of two particles. Their anomalous position is even more outspoken here.
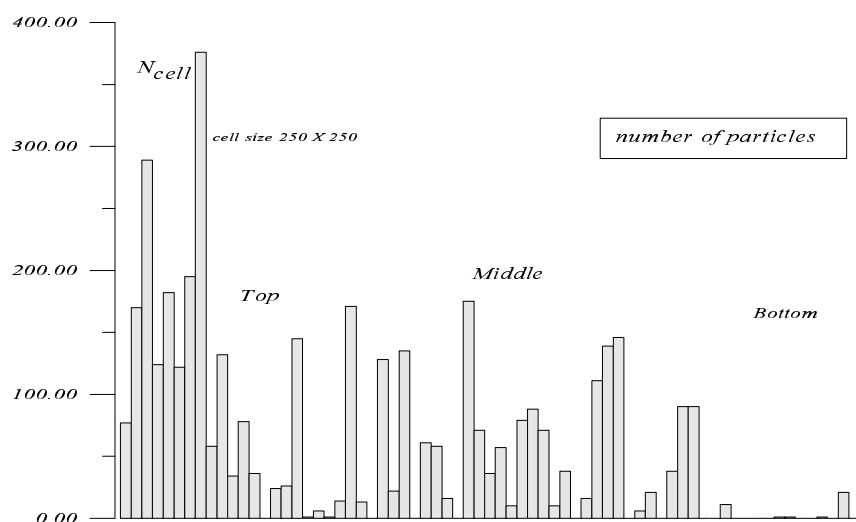
(a)
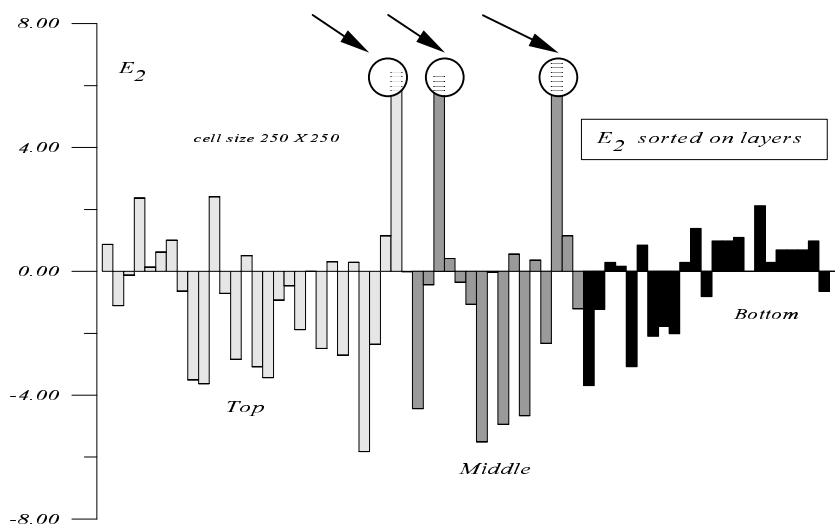
(b)

Figure 30. (a) Number of particles found in each monitoring cell. Cell size.
(b) Residuals of log-transformed concentrations for individual monitoring points.

Table 9 gives the values of E_2 as obtained with $250 \times 250 \times 10$ m^3-sized monitoring cells. The contribution of the outliers has now been discarded. Although a precise estimate of the influence of the cell size on the reliability can not be given, it is felt intuitively that the accuracy increases with the number of particles. A more sophisticated object function might be constructed based on the weighted sum of the squared residuals, where the weight is somehow related to the number of particles encountered in the monitoring cell.

Table 9   *E_1 for various runs with different half-life times*

Based on $250 \times 250 \times 10$ m^3 -sized monitoring cells

T_{50} in years	Vertical Dispersion	DF Modified	Total	Top	Middle	Bottom
2 Constant	Off	Yes	220	133	59	28
3 Constant	Off	Yes	217	122	71	24
4 Constant	Off	Yes	239	118	85	35
5 Constant	Off	Yes	278	133	97	47
6 Constant	Off	Yes	306	135	109	62
3/1 Variable	Off	Yes	209	120	62	27
5/2 Variable	Off	Yes	247	102	98	47

Breakthrough Curves

In the present study only data are considered on nitrate concentrations in the aquifer. The model can also be applied to determine breakthrough curves for nitrate in the groundwater pumping stations that are present in the area. Since for most pumping stations measured breakthrough curves are available, a comparison of calculated and measured breakthrough curves is possible and may provide useful information. At present such a comparison is being carried out within the framework of the 5th National Environmental Outlook. Results of this study will be published in a separate report.

5   CONCLUSIONS

This report focuses on the implementation of a denitrification module in the transport model
LGMCAD. A sub-area of the RIVM groundwater model has been selected for a 'pilot study'
with future application on a national scale in mind. Based on the experience gained in this work
it may be concluded that LGMCAD proves to be a useful and flexible tool to study the nitrate
distribution in deep aquifers. In the first place the problem is characterized by substantial vertical
gradients. It is well known that solute transport models based on Eulerian techniques such as the
Finite Difference Method or the Finite Element Method do not handle very well situations with
steep gradients. These methods are expected to introduce artificial (numerical) mixing over the
vertical (numerical dispersion) and, therefore, cannot produce the required vertical detail. The
advantage of Lagrangian techniques (e.g. particle tracking as applied in LGMCAD) is the
absence of numerical mixing. Furthermore, the particle concept allows for the implementation of
a simple denitrification module in the form of an exponential decay, with the rate of
denitrification expressed by the half-life time T_{50}. The decay parameter may vary both in time
and space. A less attractive feature of particle models is the necessity to discretize solute mass
by a finite number of point-masses. This introduces statistical noise and problems with
resolution. One may control these problems, to some extent, by increasing the number of
particles. At present, however, no practical guidelines exist on the optimal model behavior in
terms of the number of particles. Further research on this subject is recommended.
An alternative transport model, also a component of the LGM software package, is the program
LGMCAM (Kovar et al., 1998). LGMCAM also applies the particle concept, but contrary to
LGMCAD, it performs a particle tracking 'backward in time'. This approach is well suited to
calculate breakthrough curves in pumping well, but does not give solute concentrations in the
aquifer itself. The backward tracking method is not in favor for implementation of a
denitrification routine.

   The results of the model runs indicate that nitrate levels in the groundwater are
overestimated when denitrification is not taken into account. However, little is known on the
actual rate of denitrification in the deeper layers. Spatial variation of the denitrification
parameter has been applied based on the knowledge that presence of organic material near
separating clay layers and underneath valleys of rivers and brooks leads to faster denitrification.
The best results were obtained with a half-life time (T_{50}) of 3-5 years over the model area and a
reduction of T_{50} to 1-2 years in the vicinity of rivers and brooks and in a zone of 5 meter
thickness above and below the clay layers.

   Extra attention has been paid to processes that affect the vertical distribution of the nitrate
concentration. It appears that the fit between model results and observed data greatly improves
when vertical dispersion is reduced to the level of molecular diffusion. Application of such low
dispersivity values in the vertical direction is supported by cases from the literature. Also the
distribution of the vertical flow component has been reconsidered (advective transport). It is

known that the Dupuit-Forchheimer approach leads to an overestimation of the downward velocity. A small modification slightly improves the fit. It seems worthwhile to examine this point in more detail, since the vertical processes appear to be essential in this type of transport problems.

Analysis of the monitoring network data shows that the redox condition in the aquifer is a major factor that contributes to the variability of the nitrate content. This is not surprising as the main mechanisms for denitrification are based on oxidation of either organic matter or pyrite. Therefore, an improvement of the model performance can be expected when the spatial variability of redox conditions is somehow included. An example of such an approach is given Kinzelbach and Schäfer (1991). These authors proposed and applied a model where the simultaneous transport is considered of oxygen, nitrate, organic substrate and microbial mass.

As often in studies where simulation results and experimental data are compared, inconsistencies remain due to the scale of the sampling technique and data interpretation on the one hand and the resolution of the simulated data on the other hand. The horizontal resolution of the model (e.g. 250×250 m^2) is rather low for a meaningful comparison with the available data from the monitoring network. Processing the network data by geostatistical techniques (block kriging, see Pebesma, 1996) may lead to data that are representative for a larger volume than the original sampling volume. However, to derive meaningful averages for blocks of 250×250 m^2, one needs a denser set of measuring points than available at present.

Aspects of uncertainty and reliability in relation to the amount of particles (particle density) need to be investigated in greater detail. The efficiency of the model in terms of number of particles may be enhanced by local refinement of the particle distribution both in time and in space.

Acknowledgement

References

APPELO, C.A.J., POSTMA, D. 1993. Geochemistry, Groundwater and Pollution. Balkema, Rotterdam.

BOUMANS, L.J.M., VAN DRECHT, G. 1998. *(In Dutch)* Nitraat van het bovenste grondwater in de zandgebieden van Nederland; Een geographisch beeld op basis van de monitoring-gegevens en een vergelijking met de resultaten van procesmodellen. RIVM report 714801015, Bilthoven.

GROOTJANS, P. 1984. (*in Dutch*) De Geohydrologische Beschrijving van de Provincie Gelderland. Dienst Grondwaterverkenning TNO.

KINZELBACH, W., SCHAEFER, W. HERZER, J. 1991. Numerical modeling of natural and enhanced denitrification processes in aquifers. *Water Resources Research*. 27(6) 1123-.

KOVAR, K., LEIJNSE A., GAN, B.S. 1992. Groundwater Model for the Netherlands. Mathematical Model Development and User's Guide. RIVM Report 714305002, Bilthoven.

KOVAR, K., UFFINK, G.J.M., PASTOORS, M.J.H. 1996. Evaluation of the LGM Groundwater Model for the Netherlands for calculation of pathlines, travel times and concentration at abstraction wells. RIVM Report 703717001, Bilthoven.

KOVAR, K., PASTOORS, M.J.H., TIKTAK, A., VAN GAALEN, F.W. 1998. Application of the Netherlands Groundwater Model, LGM, for calculating concentration of nitrate and pesticides at abstraction wells in sandy soil areas of the Netherlands. RIVM Report 703717002, Bilthoven.

MAAS, C. 1980. (*in Dutch*) Macrodispersie. Resultaten van onderzoekingen te Bergambacht en Remmerden. Rapport Hyh 80-9. Rijksinstituut voor Drinkwatervoorziening, Voorburg.

MEINARDI, C.R. 1999. Private communication.

PASTOORS, M.J.H. 1992. (*in Dutch*) Landelijk Grondwater Model; conceptuele modelbeschrijving. RIVM-Report 714305004, Bilthoven.

PEBESMA, E.J., DE KWAADSTENIET. J.W. 1994. (*in Dutch*) Een landsdekkend beeld van de Nederlandse grondwaterkwaliteit op 5 tot 17 meter diepte in 1991. RIVM Report 714810014, Bilthoven.

PEBESMA, E.J., DE KWAADSTENIET. J.W. 1995. (*in Dutch*) Een landsdekkend beeld van veranderingen in de Nederlandse grondwaterkwaliteit op 5 tot 17 meter diepte. RIVM Report 714810015, Bilthoven.

PEBESMA, E.J., 1996. Mapping Groundwater Quality in the Netherlands. Ph. D. Thesis. University of Utrecht.

RAJARAM, H., GELHAR, L.W. 1991. Three-Dimensional Spatial Moments Analysis of the Borden Tracer Test. *Water Resour. Res*. 27 (6): 1239-1251.

SNELTING, H., DE BOER, J.L.M., GAST, L.F.L., KUSSE, A.A.M., WILLEMSEN, W.H. 1990. (*In Dutch*) Inrichting en exploitatie van het Landelijk Meetnet Grondwaterkwaliteit. RIVM Report 728517061, Bilthoven.

STRACK, O.D.L. 1984. Three-dimensional streamlines in Dupuit-Forchheimer models. *Water Resour. Res.* 20 (7): 812-822.

UFFINK, G.J.M. 1990. Analysis of dispersion by the random walk method. Ph. D. Thesis. Delft University of Technology.

UFFINK, G.J.M. 1996. (*In Dutch)* Landelijk Grondwater Model (LGM) Testberekeningen met een module voor stoftransport. RIVM Report 715501008, Bilthoven.

UFFINK, G.J.M. 1999. LGMCAD, a Solute Transport Module of the Groundwater Model for the Netherlands. User's Manual. RIVM Report 711401006, Bilthoven.

VAN BEEK, C.G.E.M., LAEVEN, M.P., VOGELAAR, A.J. 1994. (*In Dutch)* Modellering denitrificatie in grondwater onder invloed van organisch materiaal. H_2O (27) nr 7: 180-184.

VAN DRECHT, G., GOOSSENS, F.R., HACK-TEN-BROEKE, M.J.D., JANSEN, E.J., STEENVOORDEN, J.H.A.M. 1991. *(In Dutch)* Berekening van de nitraatuitspoeling naar het grondwater met behulp van eenvoudige modellen. RIVM Report 724901003, Bilthoven.

VAN DRECHT, G. 1993. Modelling of regional scale nitrate leaching from agricultural soils, the Netherlands. Applied Geochemistry, Suppl. Issue 2, 175-178.

VAN DRECHT, G., REIJNDERS, H.F.R., BOUMANS, L.J.M., VAN DUIJVENBOODEN, W. 1996. *(In Dutch)* De kwaliteit van het grondwater op een diepte tussen 5 en 30 meter in Nederland in het jaar 1992 en de veranderingen daarvan in de periode 1984-1993. RIVM Report 714801005, Bilthoven.

VAN DRECHT, G., SCHEPER, E. 1998. *(In Dutch)* Actualisering van model NLOAD voor nitraatuitspoeling van landbouwgronden; beschrijving van model en GIS-omgeving. RIVM Report 711501002, Bilthoven.

VAN DUIJVENBOODEN, W., TAAT, J., GAST, L.F.L. 1985. *(In Dutch)* Landelijk meetnet grondwaterkwaliteit: eindrapport van de inrichtingsfase. RIVM Report 840382001, Bilthoven,

VERMEULEN, P.T.M., STUURMAN, R.J., WITTE, J.PH.M., VAN DER MEIJDEN, R., GROEN, C.L.G. 1996. *(In Dutch)* Landelijke Hydrologische Systeemanalyse. Deelrapport 6. Het gebied ten oosten van de IJssel (Salland, etc.). TNO-Report GG-R-95-91 (B).

WENDLAND, F. 1992. Die Nitratbelastung in den Grundwasserlandschaften der 'alten' Bundesländer (BRD). Berichte aus der Ökologische Forschung. Band 8.

APPENDIX A. LOCATIONS AND MEASUREMENTS MONITORING NETWORK SAMPLING POINTS

0 - 10 m Location	Land Use	Surf. Elev. m +NAP	x-coord. m	y-coord. m	Filter depth m	NO₃ mg L⁻¹	STDEV.	#
VARSSEVELD	Urban	13.4	220878	437514	6.0	0.05	0.03	1
AALTEN	Arable	20.5	233162	437912	4.0	86.8	9.8	2
WEHL	Pasture	16.1	211873	439240	4.0	48.9	6.2	3
GAANDEREN	Pasture	14.0	220985	439775	9.1	0.03	0.02	4
DIDAM	Arable	12.0	206135	440370	8.0	16.2	1.0	5
HEELWEG	Pasture	19.0	229020	442700	9.4	0.04	0.02	6
DOETINCHEM	Urban	15.7	217477	443233	7.0	13.9	0.6	7
LICHTENVOORDE	Pasture	19.4	231720	443954	4.0	0.05	0.03	8
LICHTENVOORDE	Arable	30.1	238907	444465	4.0	53.2	3.2	9
HUMMELO	Forest	13.8	215648	445107	7.0	0.6	0.9	10
ZELHEM	Pasture	18.4	226350	445776	4.0	0.1	0.1	11
ANGERLO	Irrelevant	9.0	207975	445925	8.9	0.05	0.02	12
ZELHEM	Forest	18.2	224397	446956	4.0	0.9	0.3	13
HUMMELO	Arable	11.0	212975	447260	9.0	37.4	8.3	14
LIEVELDE	Pasture	18.0	235915	447710	9.0	0.05	0.01	15
ZELHEM	Arable	17.0	220602	448451	4.0	19.0	2.6	16
KEYENBORG	Arable	15.0	218750	449190	8.9	49.7	3.5	17
VELDHOEK	Forest	7.0	222795	450795	9.0	5.2	2.4	18
HENGELO	Pasture	17.2	225037	450920	4.0	10.5	8.9	19
GROENLO	Urban	23.9	238756	451033	3.8	30.3	5.0	20
STEENDEREN	Arable	10.2	210461	454015	7.0	63.9	33.8	21
EIBERGEN	Pasture	20.0	239180	456700	9.5	0.04	0.01	22
EERBEEK	Arable	12.2	203937	458055	4.5	56.1	4.7	23
VORDEN	Forest	13.0	221560	459680	9.0	6.8	2.5	24
WARNSVELD	Pasture	8.0	211975	461935	8.6	0.03	0.03	25
WARNSVELD	Forest	10.7	218074	462392	9.0	0.05	0.06	26
KLARENBEEK	Pasture	8.0	202825	463263	7.1	0.03	0.03	27
NOORDIJK	Pasture	14.0	235385	463315	8.1	0.03	0.03	28
LOCHEM	Urban	14.4	224916	463865	6.0	19.2	6.2	29

10 - 20 m Location	Land Use	Surf. Elev. m +NAP	x-coord. m	y-coord. m	Filter depth m	NO₃ mg L⁻¹	STDEV.	#
BERGH	Forest	26.9	212254	437509	14	24.1	7.9	1
VARSSEVELD	Urban	13.4	220878	437514	15.8	0.33	0.26	2
AALTEN	Arable	20.5	233162	437912	14	0.14	0.22	3
DIDAM	Arable	12.0	206135	440370	18.9	18.0	4.0	4
DOETINCHEM	Urban	15.7	217477	443233	14	1.5	0.9	5
HUMMELO	Forest	13.8	215648	445107	14	0.09	0.08	6
ZELHEM	Pasture	18.4	226350	445776	14	0.11	0.04	7
ZELHEM	Forest	18.2	224397	446956	14.8	16.4	3.3	8
ZELHEM	Arable	17.0	220602	448451	14	46.7	22.4	9
HENGELO	Pasture	17.2	225037	450920	14	0.03	0.02	10
ELLECOM	Forest	30.8	201673	451254	14.5	5.4	1.5	11
LAAG-SOEREN	Forest	19.0	201415	454755	11	0.07	0.01	12
RUURLO	Urban	17.0	227450	456260	10.9	0.06	0.04	13
EERBEEK	Arable	12.2	203937	458055	14	0.05	0.05	14
WARNSVELD	Forest	10.7	218074	462392	14	0.13	0.21	15
LOCHEM	Urban	14.4	224916	463865	14	25.7	1.8	16

20 - 30 m Location	Land Use	Surf. Elev. m +NAP	x-coord. m	y-coord. m	Filter depth m	NO$_3$ mg L^{-1}	STDEV.	#
HENGELO	Pasture	17.2	225037	450920	24.0	0.02	0.02	1
KLARENBEEK	Pasture	8.0	202825	463263	24.0	0.03	0.01	2
LOCHEM	Urban	14.4	224916	463865	24.0	0.03	0.02	3
ZELHEM	Pasture	18.4	226350	445776	24.0	0.04	0.03	4
WARNSVELD	Forest	10.7	218074	462392	24.0	0.04	0.04	5
AALTEN	Arable	20.5	233162	437912	24.0	0.04	0.04	6
HUMMELO	Arable	11.0	212975	447260	24.4	0.05	0.04	7
NOORDIJK	Pasture	14.0	235385	463315	24.6	0.06	0.02	8
HEELWEG	Pasture	19.0	229020	442700	23.9	0.06	0.03	9
RUURLO	Urban	17.0	227450	456260	24.7	0.06	0.02	10
LAAG-SOEREN	Forest	19.0	201415	454755	26.0	0.06	0.01	11
VELDHOEK	Forest	7.0	222795	450795	24.0	0.07	0.06	12
KEYENBORG	Arable	15.0	218750	449190	23.6	0.07	0.03	13
LIEVELDE	Pasture	18.0	235915	447710	24.0	0.08	0.03	14
VARSSEVELD	Urban	13.4	220878	437514	24.0	0.08	0.10	15
DOETINCHEM	Urban	15.7	217477	443233	24.0	0.08	0.12	16
EIBERGEN	Pasture	20.0	239180	456700	23.0	0.08	0.03	17
WARNSVELD	Pasture	8.0	211975	461935	24.0	0.09	0.13	18
VORDEN	Forest	13.0	221560	459680	24.0	0.12	0.06	19
ANGERLO	Irrelevant	9.0	207975	445925	24.4	0.12	0.11	20
GAANDEREN	Pasture	14.0	220985	439775	24.1	0.25	0.34	21
ZELHEM	Arable	17.0	220602	448451	24.0	1.91	3.11	22
BERGH	Forest	26.9	212254	437509	24.0	2.57	3.08	23
ELLECOM	Forest	30.8	201673	451254	24.0	3.49	2.88	24

APPENDIX B. CADFILES

Example of cadfile for Run without denitrification

```
Nitrate transport Achterhoek; no decay (denitrification)

[TIMES]
15000, 250                                 final time and timestep


[OUTPUT]
cloud
4, 1                                       # clouds + offset
3750, 7300, 10950, 14600
0                                          # monitoring wells

[PROCESS-PARAMETERS]
10.000 1.00000 1.00000                     dispersivities
0                                          number of changes
1
1.                                         retardation-factor
0                                          idecay

[RELEASE-RATES]
0                                          # locations for release
7, 10                                      # files for grid release, type
0.00273973                                 (1/365) conversion year to day

; the following (7) files contain release rates
; 'filename',time, number of pulses, number of particles

'/home/lbg/lbguffi/lgm/nitraat/gasfiles/redux50.g2a', 0, 20 , 20000
'/home/lbg/lbguffi/lgm/nitraat/gasfiles/redux60.g2a', 3650, 20 ,30000
'/home/lbg/lbguffi/lgm/nitraat/gasfiles/redux70.g2a', 7300, 20, 35000
'/home/lbg/lbguffi/lgm/nitraat/gasfiles/redux80.g2a', 10950, 20 , 35000
'/home/lbg/lbguffi/lgm/nitraat/gasfiles/redux90.g2a', 14600, 10 , 30000
'/home/lbg/lbguffi/lgm/nitraat/gasfiles/redux95.g2a', 16425, 20 , 10000
'/home/lbg/lbguffi/lgm/nitraat/gasfiles/copred95.g2a', 20000, 1 , 0
1
200000, 435000, 240000, 465000


[MISCELANEOUS]
2                                          seed for random generator
1
200000, 240000, 435000, 465000
.5                                         reduction number of particles
[END]
```

Example of cadfile for case with constant decay ($T_{50} = 5$ years)

```
Nitrate transport Achterhoek ; Decay ~ 5 years

[TIMES]
17500, 250                                    final time and timestep

[OUTPUT]
cloud
4, 1                                          # clouds + offset
3750, 7300, 10950, 14600
0                                             # monitoring wells

[PROCESS-PARAMETERS]
10.000 1.00000 1.00000                        dispersivities
0                                             number of changes
1
1.                                            retardation-factor
2                                             idecay
1721

[RELEASE-RATES]
0                                             # locations for release
7, 10                                         # files for grid release
0.00273973                                    (1/365) conversion year to days


; the following (7) files contain release rates
; 'filename',time, number of pulses, number of particles


'/home/lbg/lbguffi/lgm/nitraat/gasfiles/redux50.g2a', 0, 20 , 20000
'/home/lbg/lbguffi/lgm/nitraat/gasfiles/redux60.g2a', 3650, 20 ,30000
'/home/lbg/lbguffi/lgm/nitraat/gasfiles/redux70.g2a', 7300, 20, 35000
'/home/lbg/lbguffi/lgm/nitraat/gasfiles/redux80.g2a', 10950, 20 , 35000
'/home/lbg/lbguffi/lgm/nitraat/gasfiles/redux90.g2a', 14600, 10 , 30000
'/home/lbg/lbguffi/lgm/nitraat/gasfiles/redux95.g2a', 16425, 20 , 10000
'/home/lbg/lbguffi/lgm/nitraat/gasfiles/copred95.g2a', 20000, 1 , 0
1
200000, 435000, 240000, 465000


[MISCELANEOUS]
2                                             seed for random generator
1
200000, 240000, 435000, 465000
.5                                            reduction number of particles
[END]
```

Example of cadfile for variable decay

```
Nitrate transport Achterhoek, 3 layers denitrification (5 years/2 years)

[TIMES]
17500, 250                                      final time and timestep

[OUTPUT]
cloud
4, 1                                            # clouds + offset-parm
3750, 7300, 10950, 14600
0                                               # monitoring wells

[PROCESS-PARAMETERS
10.000 1.00000 1.00000                          dispersivities
0                                               # of changes
1
1.                                              retardation-factor
6                                               idecay
1825
3                                               # denitrification layers

; definition of three layers with variable decay parameter

TOPSYS.GRD                                       elevation top first layer
BEEKT5.GRD                                       decay parameters in first layer
TOPCLAYP5.GRD                                    elevation top second layer
BKKLEI5.GRD                                      decay parameters second layer
BOTCLAYM5.GRD                                    elevation top of third layer
BEEKB5.GRD                                       decay parameters third layer
BOTSYS.GRD                                       elevations bottom third layer


[RELEASE-RATES]
0                                               # locations for release
7, 10                                           # files for grid release
0.00273973                                      (1/365) conversion year to days

; the following (7) files contain release rates
; 'filename',time, number of pulses, number of particles

'/home/lbg/lbguffi/lgm/nitraat/gasfiles/redux50.g2a', 0, 20 , 20000
'/home/lbg/lbguffi/lgm/nitraat/gasfiles/redux60.g2a', 3650, 20 ,30000
'/home/lbg/lbguffi/lgm/nitraat/gasfiles/redux70.g2a', 7300, 20, 35000
'/home/lbg/lbguffi/lgm/nitraat/gasfiles/redux80.g2a', 10950, 20 , 35000
'/home/lbg/lbguffi/lgm/nitraat/gasfiles/redux90.g2a', 14600, 10 , 30000
'/home/lbg/lbguffi/lgm/nitraat/gasfiles/redux95.g2a', 16425, 20 , 10000
'/home/lbg/lbguffi/lgm/nitraat/gasfiles/copred95.g2a', 20000, 1 , 0
1
200000, 435000, 240000, 465000


[MISCELANEOUS]
2                                               seed for random generator
1
200000, 240000, 435000, 465000
.5                                              reduction number of particles
[END]
```

APPENDIX C. Dupuit-Forchheimer Approximation

In general, when flow enters an aquifer at the top there still is a vertical flow component at some depth from the top. The vertical component q_z gradually decreases with depth until it becomes zero at the base of the aquifer, assuming that the base is impervious. In the Dupuit-Forchheimer approach the distribution of q_z is a linear function with depth. If the vertical flow is N at the top of the aquifer ($q_z = N$ for $z = H$) and zero at the bottom ($q_z = 0$ for $z = 0$), then one can write:

$$q_z = N f(z)$$

where in the case of Dupuit-Forchheimer :

$$f(z) = \frac{z}{H}$$
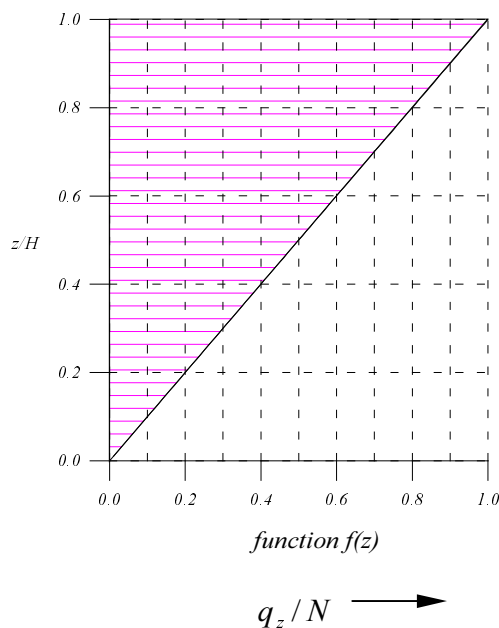
Fig C-1. *Vertical distribution of q_z according to Dupuit-Forchheimer.*

The linear function is a simplification. It would be true only if the vertical permeability is infinitely high (no resistance to vertical flow). With a finite permeability (or a positive resistance to flow) the decrease of q_z is expected to be faster in the upper part of the aquifer and slower in the lower part. When *f(z)* is seen as a first order approximation, we may try second order

approximations by slightly modifying *f(z)*. A natural extension is to add a second quadratic function *g(z),* such that we can write $q_z = N\big(f(z) + \beta\, g(z)\big)$. An example for *g(z)* is:

$$g(z) = \frac{z}{H}\left(\frac{z}{H} - 1\right)$$
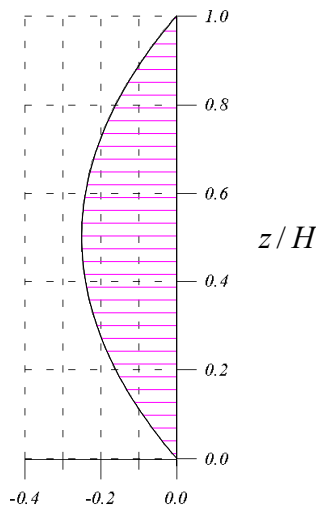
Fig C-2 Example quadratic function g(z)

The function *g(z)* is zero at the top and the bottom of the aquifer and, therefore, does not conflict with the vertical boundary conditions ($q_z = N$ for *z = H* ; $q_z = 0$ for *z = 0*). Half-way the aquifer *g(z) = -1/4*. Note that *g(z)* is negative for all values of *z* between 0 and *H*. This means indeed a faster decrease of q_z in the upper part of the aquifer. For $\beta = 1$ q_z reduces to:

$$q_z = N\left(\frac{z}{H}\right)^2$$

Several other vertical distributions may be constructed using other values for β. Values greater than 1 however, are not appropriate since this results in a distribution with upward and downward velocities which does not make sense in a situation with infiltration at the top and an impervious base at the bottom.

For the simulations in this report we have used a multiplication faction $\beta = 1/2$, so q_z becomes:

$$q_z = N\left(\frac{z}{H} + \frac{1}{2}\frac{z}{H}\frac{z-H}{H}\right)$$
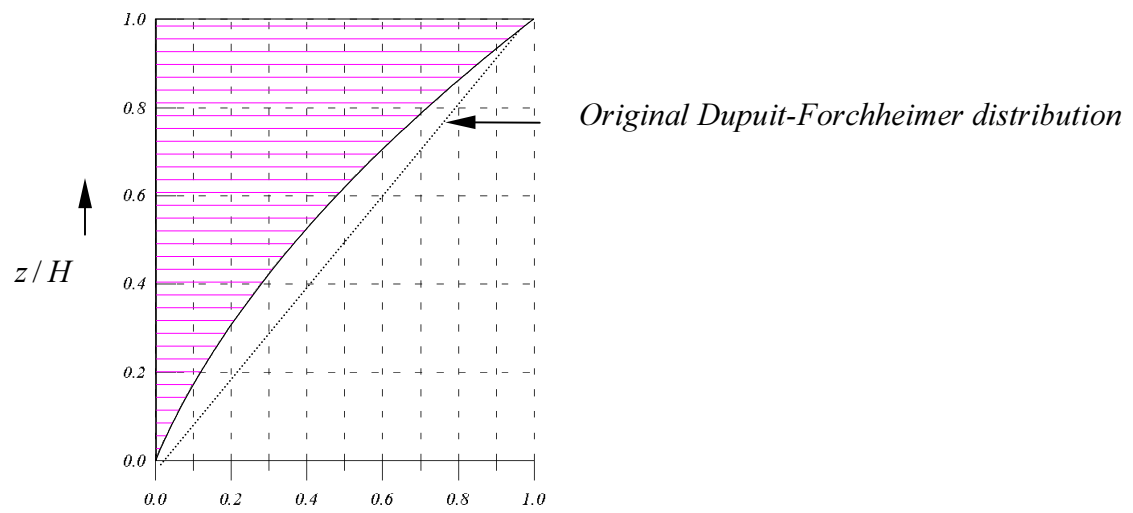
Fig C-3 Modified distribution of vertical velocity component.